# III

# ELECTRICAL PROPERTIES OF TISSUE

# 6

# Electrical Properties of Biological Tissue

**RONALD PETHIG**

Institute of Molecular and Biomolecular Electronics
University College of North Wales
Bangor, United Kingdom

## INTRODUCTION

Increasing attention is being given to investigations of the electrical properties of biological materials. There are several reasons for this, which include an increasing awareness of the possible physiological effects associated with the absorption by tissues of electromagnetic fields (1-5). Studies of the ways in which tissues interact with electromagnetic energy are also important in the continuing developments in radiofrequency and microwave hyperthermia (6, 7), impedance pneumography (8), impedance plethysmography (9), electrical impedance tomography (10, 11), the thawing of cryogenically preserved tissue (12), and in the use of pulsed electric and magnetic fields to aid tissue and bone healing (13).

Measurements of the electrical properties of biological materials have provided important contributions to the biophysical and physiological sciences. For example, Höber (14) measured the electrical impedance of red blood cell suspensions up to 10 MHz and, finding that their impedance decreased with increasing frequency, concluded that the cells were surrounded by a poorly conducting membrane and that they contained a cytoplasm of relatively low resistivity. Among the first indications of the ultra-thin nature of this membrane were those provided by Fricke (15) who obtained a value of 0.81 $\mu F/cm^2$ for the red blood cell membrane. On assuming a value of 3 for the dielectric constant of the membrane material, Fricke derived a membrane thickness of 3.3 nm. Quantitative details of the molecular size, shape and hydration content of protein molecules were provided by the dielectric measurements of Oncley (16), and these were extended in the laboratories of Hasted (17), Grant (18), and Schwan (19) to provide more details of the physical nature of protein hydration. As examples of how electrical and dielectric studies continue to provide new knowledge to the biophysical and physiological sciences, we can quote the studies of the diffusional motions of lipids and proteins in cell membranes by Kell and Harris (20), the field-induced cell rotation studies of Zimmermann's laboratory (21), studies of the influence of hydration on enzyme activation and molecular mobility (22), and of protonic and ionic charge transport processes in protein structures (23, 24).

In this Chapter we shall be concerned with the parameters that influence the way in which biological materials interact with nonionizing electromagnetic (EM) radiation. Since EM radiation is composed of electric and magnetic fields, we need in principle to consider not only the electrical parameters such as conductivity and permittivity, but also the magnetic permeability. However, apart from materials of the form of magnetite, which is known to be associated with orientational and navigational sensing abilities of some bacteria, insects and mammals (25), most biological materials have a permeability close to that of free space. Magnetic fields are also able to interact with the nuclear magnetic moments or with unpaired electrons associated with paramagnetic ions or free radical species. Such interactions are highly specific and in general have very little influence on bulk electrical properties. In this way, we shall be primarily concerned with the dielectric and electrical conduction properties of biological materials, and in particular with variations of the relative permittivity and conductivity as a function of frequency. A full historical account of the field of study cannot be attempted here, but may be derived from several texts (26-28). A full description of the electrical properties of cells and tissue should ideally include details associated with active ion transport and membrane potentials, but we shall mainly be concerned here with the so-called passive electrical parameters. Relevant aspects of other tissue electrical properties can be found elsewhere (29-31). Finally, valuable tabulations of the dielectric properties of various tissues and biomaterials have already been formulated by Geddes and Baker (32) and by Stuchly and Stuchly (33). An update of these last two reports is attempted here, together with an overview of the present theories which have been formulated in an effort to understand the electrical properties in terms of the underlying physical and physiological processes involved.

## DIELECTRIC THEORY: A SUMMARY

The electrical properties of a material held between two parallel electrodes of area $A$ and separation $d$ can be completely characterized by its electrical conductance $G$ and capacitance $C$, as defined in the following two equations:

$$G = \sigma A/d \qquad \text{and} \qquad C = A\varepsilon_0 \varepsilon/d \tag{1}$$

The conductivity σ is the proportionality factor between electric current and electric field, and is a measure of the ease with which delocalized charge carriers can move through the material under the field's influence. For biological materials, the conductivity arises mainly from the mobility of hydrated ions. The factor $\varepsilon_0$ is the dielectric permittivity of free space ($8.854 \times 10^{-12}$ F/m) and $\varepsilon$ is the material's permittivity relative to free space, sometimes referred to as the dielectric constant. The permittivity is the proportionality factor between electric charge and the electric field, and it reflects the extent to which localized charge distributions can be distorted or polarized under the influence of the

field. For biological materials such charges are mainly associated with electrical double layers occurring at membrane surfaces or around solvated macromolecules, or with polar molecules which by definition possess a permanent electric dipole moment. Examples of electrical double layers at a cell membrane surface and around a globular protein, as well as of a molecular dipole, are shown in Figure 1. The simplest molecular dipole consists of a pair of electrical charges $+q$ and $-q$ separated by a vector distance $s$, and in this case the dipole moment m is given as $m = qs$. For a protein molecule such as that shown in Figure 1, positive and negative charges arise from the presence of ionizable acidic and basic amino-acid side chains in the protein structure, and these will give rise to a comparatively large dipole moment whose value will vary with pH and molecular conformation.

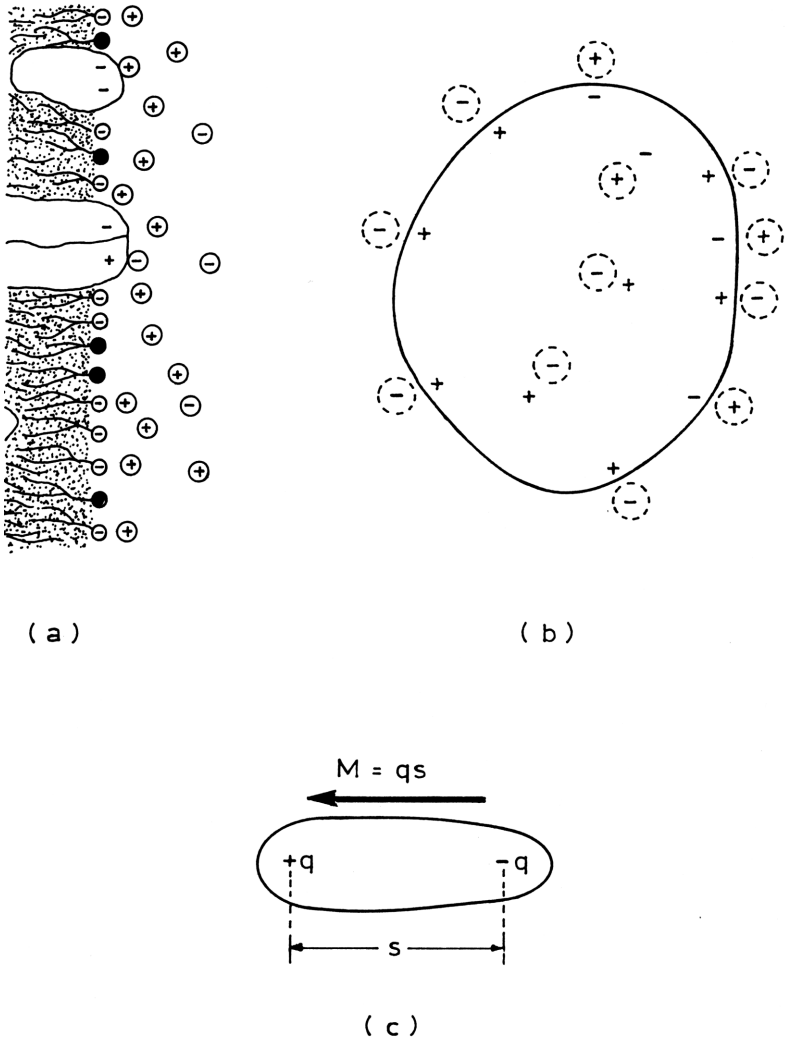


**Figure 1.** (a) Electrical double layers formed at the surface of a membrane and (b) around a globular protein. (c) A simple polar molecule of dipole moment M.

Each type of polarizable entity will exhibit its own characteristic temporal response to an imposed electric field and this is mathematically handled by describing the relative permittivity as a complex function of the form:

$$\varepsilon^*(\omega) = \varepsilon_\infty + \left(\varepsilon_s - \varepsilon_\infty\right)/\left(1 + i\omega\tau\right) \tag{2}$$

in which $\varepsilon_\infty$ is the permittivity measured at a sufficiently high frequency for the polarizable entity to be unable to respond to the electric field, $\varepsilon_s$ is the limiting low frequency permittivity where the polarization effect is fully realized, $\omega$ is the angular frequency, $i$ is $\sqrt{-1}$ and $\tau$ is the characteristic response or relaxation time. The real and imaginary components of the relative permittivity can be expressed in the form:

$$\varepsilon^* = \varepsilon' - i\varepsilon''$$

in which the real part $\varepsilon'$, corresponding to the permittivity parameter in Equation (1), is given by:

$$\varepsilon'(\omega) = \varepsilon_\infty + \left(\varepsilon_s - \varepsilon_\infty\right)/\left(1 + \omega^2\tau^2\right) \tag{3}$$

The imaginary component $\varepsilon''$, corresponding to the dissipative loss associated with the polarizable charges moving in phase with the electric field, is given by:

$$\varepsilon''(\omega) = \left(\varepsilon_s - \varepsilon_\infty\right)\omega\tau/\left(1 + \omega^2\tau^2\right) \tag{4}$$

and takes the form of a loss peak as shown in Figure 2 for water. The loss factor $\varepsilon''$ can also be defined in terms of a frequency-dependent conductivity as:

$$\varepsilon'' = \sigma(\omega)/\omega\varepsilon_0 = \left(\sigma_0 + \sigma_d(\omega)\right)/\omega\varepsilon_0$$

where $\sigma_0$ is the steady-state conductivity arising mainly from mobile ions, and $\sigma_d(\omega)$ is the frequency-dependent conductivity arising from dielectric polarization losses.

A more useful form of the above equations can be derived from defining the magnitude of the dielectric dispersion as:

$$\Delta\varepsilon = \varepsilon_s - \varepsilon_\infty$$

From Equations (3) and (4) we then obtain the relationships:

$$\varepsilon'(\omega) = \varepsilon_\infty + \Delta\varepsilon/\left(1 + \left(f/f_r\right)^2\right) \tag{5}$$

and

$$\sigma(\omega) = \sigma_s + 2\pi\varepsilon_0 f^2 \Delta\varepsilon \Big/ f_r\left(1 + \left(f/f_r\right)^2\right) \tag{6}$$

in which $f_r$ is the relaxation frequency $\left(f_r = 1/2\pi\tau\right)$. The factor $\sigma_s$ is the low-frequency limit of the conductivity that includes the steady-state conductivity and dielectric losses associated with any polarization processes having relaxation frequencies well below that defined by $f_r$ above. For frequencies very much greater than $f_r$, from Equation (6) we have:

$$\Delta\sigma = \sigma_\infty - \sigma_s = 2\pi\varepsilon_0 f_r \Delta\varepsilon \tag{7}$$

This shows that the increment in conductivity is directly proportional to the permittivity change and can be used as a check on the validity of experimental data. We can also write Equation (6) in the form:

$$\tau = \varepsilon_0 \Delta\varepsilon / \Delta\sigma$$

and this is a relationship that holds reasonably well for the case where the polarizable entity exhibits a spread of relaxation tines.

A simple model, which can be used to describe dielectric relaxation processes that involve dipolar molecules, is one that considers the dipoles to be spheres whose rotation is opposed by the viscosity of the surrounding medium. The relevant relaxation time for such a sphere is given by:

$$\tau = \xi / 2kT$$

where $\xi$ is a molecular friction constant that relates the torque exerted on the dipole molecule by the external electric field to the molecule's angular velocity, $k$ is Boltzmann's constant and $T$ is the absolute temperature. Assuming the dipole molecule to be equivalent to a rigid sphere of radius $a$ turning in a hydrodynamic fluid of macroscopic viscosity $\eta$, then using Stokes' law we have:

$$\xi = 8\pi\eta a^3$$

This gives the relaxation time as:

$$\tau = 4\pi\eta a^3 / kT \tag{8}$$

Considering the simple nature of the model used, Equation (8) gives surprisingly good results, even for the case of water molecules rotating in bulk water. The distance between adjacent oxygen molecules in bulk water is 0.28 nm, so we can take the molecular radius of water to be one-half of this, namely 0.14 nm. At 293°K the viscosity of water is $10^{-3}$ kg/msec and the value for the relaxation time derived from Equation (8)

is $8.5 \times 10^{-12}$ sec, in close agreement with the experimental value of $9.3 \times 10^{-12}$ sec. This relaxation time is equivalent to a relaxation frequency of 17 GHz, and the frequency-dependencies of $\varepsilon'$ and $\varepsilon''$ for bulk water at 293°K are shown in Figure 2(a). The corresponding increase in the conductivity of pure water, from its low-frequency value of $5 \times 10^{-6}$ mho/m, is shown in Figure 2(b). The low-frequency conductivity of biological electrolytes (equivalent to 150 mM saline solution) is around 2 mho/m, and above 2 GHz their conductivities exhibit approximately the same frequency dependencies as the curve shown in Figure 2(b).

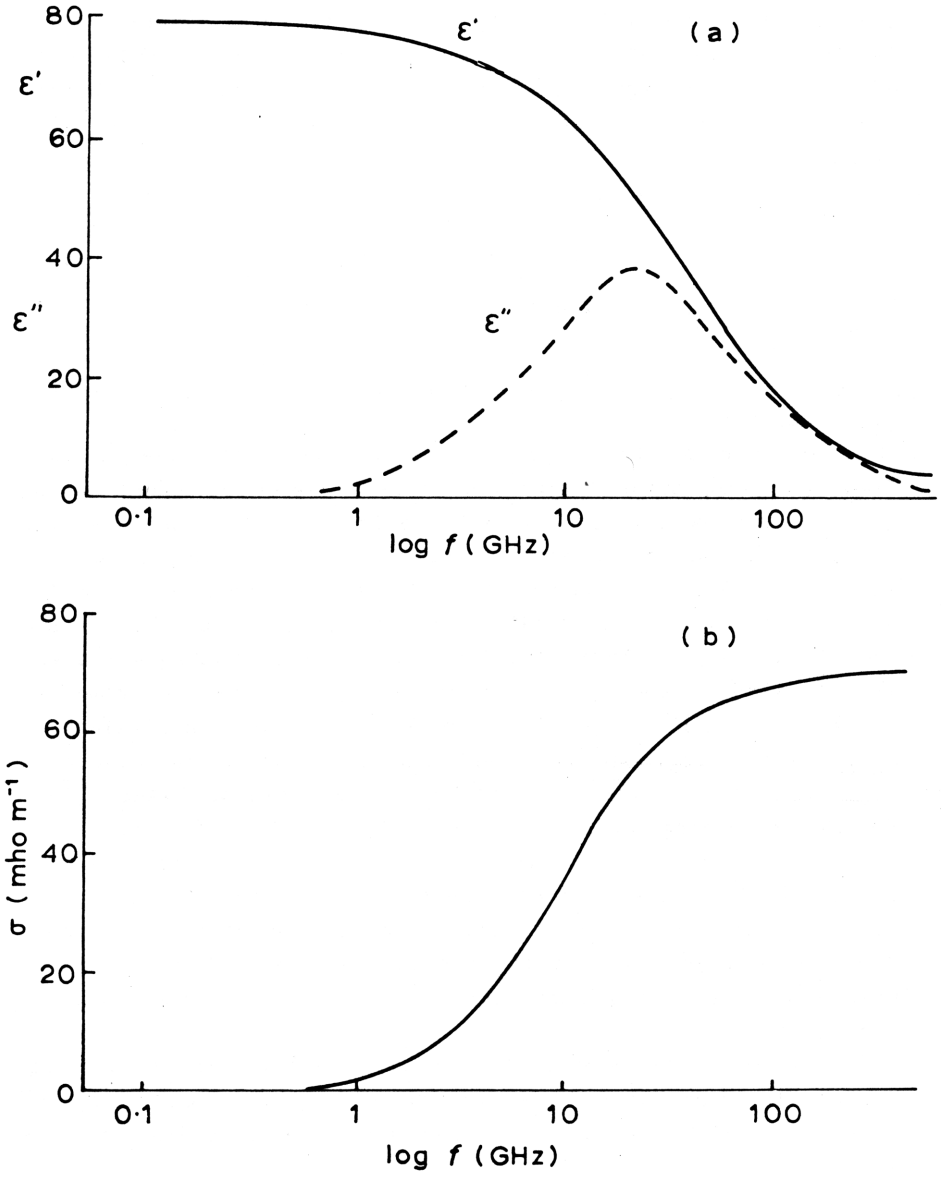


**Figure 2.** (a) The dielectric dispersion and loss peak for pure water at room temperature. (b) The associated increase in the conductivity of pure water from its low frequency value of $5 \times 10^{-6}$ mho/m.

Following the work of Kirkwood (34, 35) we can relate the dielectric dispersion

strength to the dipole moment *m* and molecular weight *M* of the polar molecule according to the relationship:

$$\Delta\varepsilon = NCgm^2 / 2\varepsilon_0 MkT \tag{9}$$

where *N* is Avogadro's number and *C* is the concentration (kg/m$^3$) of the polar molecule in the solvent. The parameter *g* was introduced by Kirkwood to take account of molecular associations and correlation effects between the solute and solvent molecules. Such effects are particularly large for hydrogen-bonded liquids such as water, where the rotation of one water molecule disrupts the local hydrogen bonding and requires, as compensation, the correlated reorientation of four or more neighboring water molecules. For water at room temperature, *g* is 2.8, and it drops to around 2.5 at l00°C. A value for *g* of unity implies no molecular associations, and this situation is usually approached with increasing molecular weight of the polar solvent molecule. In the next section we shall see that for α-amino acids *g* has an estimated value of around 1.2. For globular proteins in aqueous solution it is usually assumed that *g* has a value of unity. Sometimes the polar molecules are rotationally hindered, and this can give rise to a value for *g* of less than unity. This effect can occur in different cases including polar side-chains in protein structures, proteins partially immobilized in membranes, or water strongly associated (bound) with protein or membrane surfaces.

Hopefully, this brief outline of dielectric polarization processes and theory will aid those whose specializations lie outside the subject to more fully appreciate the dielectric topics described in this Chapter. More comprehensive treatments of dielectric theory of relevance to biological materials can be found in Grant et al. (26) and Pethig (27).

## AMINO ACIDS, PROTEINS AND DNA

### AMINO ACIDS

The term amino acid could be used to refer to any compound that contains amino and acidic groups, but it is usually considered to mean the α-amino carboxylic acids isolated from natural sources. Well over 100 of these have been isolated, but only 20 are commonly obtained upon hydrolysis of proteins. These acids contain an amino group in a position alpha to a carboxyl group and can be represented by the following chemical structure:

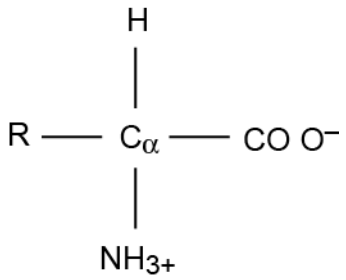


where R is the variable side chain characterizing the particular amino acid. The side chains largely determine the dielectric properties of proteins, The structure above is shown in the form that exists in aqueous solutions at neutral pH, in which the carboxylic acid and amino groups are ionized. One consequence of this is that the process of solvation of amino acids in water is accompanied by a strong negative volume change, resulting from the electrostatic forces of attraction between the polar water molecules and the two charged groups. Also, because the ionized form (zwitterion) represents a large dipole, neutral solutions of amino acids have high permittivities. Amino acids in neutral solution absorb infra-red radiation at 1580 $cm^{-1}$, which is characteristic of the CO $O^-$ carboxylate ion, and not at 1710 $cm^{-1}$ as would be the case for a nonionized carboxyl group. We shall refer to this again when considering the properties of protein-associated water.

The simplest amino acid is glycine, for which the side chain R is one hydrogen atom. From a straight forward structural model of this molecule, the distance *d* between the positive charge on the nitrogen atom of the amino group and that of the negative charge shared between the oxygen atoms of the carboxyl group should be about 0.32 nm. The effective dipole moment should then have a value given by:

$$m = qs = \left(1.6 \times 10^{19}\right) \times \left(3.2 \times 10^{-10}\right) = 5.1 \times 10^{-29} C \bullet m = 15.3 \text{ Debye units.}$$

This value-compares reasonably well with the early estimate by Wyman (36) of 20 Debye units obtained from dielectric measurements. Dunning and Shutt (37) found that the permittivity of glycine solutions is constant from pH 4.5 to pH 7.5, but falls sharply on both sides of this pH range. This is another consequence of the dipolar ionic form of α-amino acids. At the lower pH values the carboxyl group will tend not to be ionized, and likewise for the amino group at the high pH range, so that the polar form will disappear in acid or alkali solutions. In the polar, zwitterion, form the dipole moment per unit volume of an α-amino acid is larger than that of a water molecule, and amino acid solutions therefore exhibit a greater permittivity than that of pure water, as can be seen for glycine in Figure 3. At room temperature the dielectric dispersion for glycine solutions is centered around 3.3 GHz (26), and it overlaps with the dispersion for water (Figure 3). Because of the large electrostatic interactions that occur between the charged carboxyl and amino groups and the surrounding water dipoles, the model used to derive

Equation (8) is not valid (a relaxation frequency of 12.5 GHz is predicted from Equation (8)). In fact, no straightforward theoretical interpretation of the dielectric dispersion of amino acid solutions has been forthcoming. The molecular polarizabilities of amino acid solutions have often been expressed in the form:

$$\varepsilon = \varepsilon_1 + \delta c \tag{10}$$

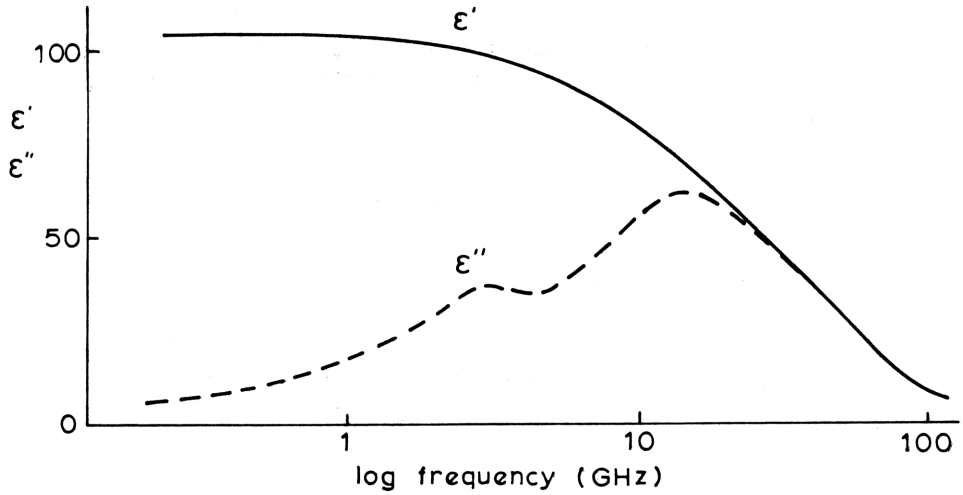


**Figure 3.** The dielectric dispersion of a 1 M aqueous glycine solution. The low-frequency permittivity is greater than that of pure water and the dispersions for glycine and water overlap.

where $\varepsilon$ and $\varepsilon_1$ are the permittivities of the solution and pure solvent respectively, and $c$ is the molar concentration of the solute. The specific dielectric increment $\delta$ is given by:

$$\delta = \Delta\varepsilon / c$$

and quantifies the increase in polarizability. For low concentrations $\delta$ is usually found to be constant, so that the measured permittivity varies linearly with concentration. For aqueous solutions of α-amino acids at 25°C, $\delta$ is 26–28 for frequencies up to 1 GHz and concentrations up to 2.5 M. Taking the dipole moment of 15.3 D obtained for glycine as being typical, a value for $g$ of around 1.2 can be estimated (from Equation (9)) for aqueous α-amino acid solutions.

## POLYPEPTIDES AND PROTEINS

The way in which linear chains of amino acids, called polypeptide chains, are built up by the formation of peptide bonds is shown in Figure 4(a) . These peptide bonds take the form of an amide linkage between α-amino and α-carboxyl groups of adjacent amino acids. For each linkage formed there is the loss of one water molecule, so polypeptide chains are in fact formed of amino acid residues. As the polypeptide increases in length,

the distance between the terminal carboxyl and amino charges also tends to increase and along with it the effective dipole moment and observed dielectric increment. For polypeptide chains up to glycine heptapeptide, the specific dielectric increment varies linearly according to the relationship:

$$\delta = 14.51(n) - 5.87$$

where $n$ is the number of chemical bonds between the terminal carboxyl and amino group (27).

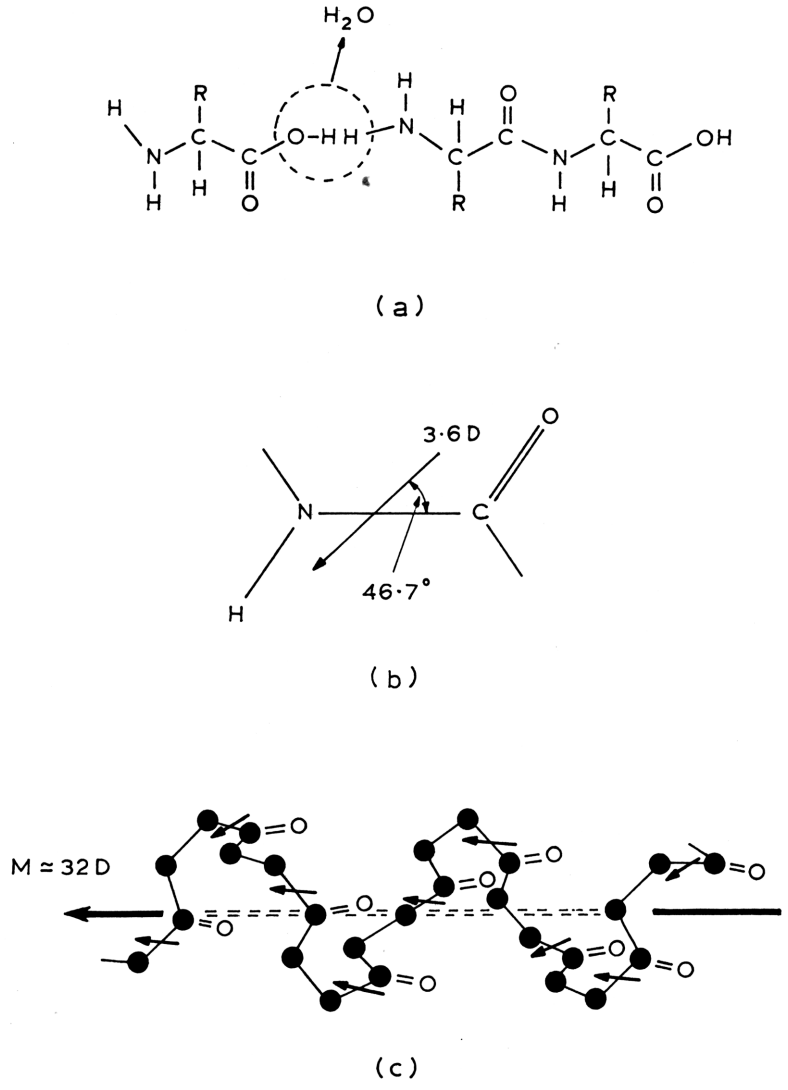


**Figure 4.** (a) The formation of peptide bonds to form a polypeptide chain. (b) The dipole moment of a peptide unit. (c) The individual peptide moments are additive in an alpha-helix.

Protein molecules are composed of one or more polypeptide chains, and the three-dimensional structure of proteins is influenced by the way some of the peptide units link

with one another to form regions of α-helical or pleated β-sheet configurations. The N–C bond in the peptide units has partial double-bond character and as a result the six atoms $C_\alpha NHCOC_\alpha$ are coplanar. Also, the C–O bond is polar and this is largely responsible for the peptide unit possessing a permanent dipole moment. A relatively straightforward quantum mechanical calculation (27) (pp. 44–49) gives the magnitude of this dipole moment as being around 3.6 D and directed at an angle of 46.7° to the C–N bond axis (Figure 4(b)). Since each peptide unit possesses a permanent dipole moment, then polypeptide chains effectively take the form of strings of connected dipoles. The contribution that a dipole of moment $m$ makes to the polarizability of a medium is proportional to $m^2$. For a completely rigid linear polymer chain of $n$ regularly spaced dipolar units of moment $m$, fixed and directed normal to the chain, the total contribution to the polarizability will either be zero or of the order of ($nm^2$), depending upon whether the dipoles vectorially cancel or are additive. If these dipolar units are perfectly free to rotate, the contribution will be $nm^2$. For most polypeptide systems, $n$ will typically be $10^2$–$10^3$, so that the peptide unit dipole contribution to the overall dipole moment value of the protein molecule, and hence to the permittivity of an aqueous protein solution, could be extremely sensitive to the polypeptide configuration.

A good example of where the peptide group moments are totally additive is the extended α-helix configuration depicted in Figure 4(c). The axis of a rigid polypeptide α-helix is directed at about 56° to the C–N bond of the constituent peptide units. Since the peptide dipole moment is directed at 46.7° to the C–N bond, the peptide contribution to the total moment parallel to the helix will be:

$m_{11} = 3.6n\ \mathrm{Cos}(9.3°) = 3.6n$ Debye units.

The α-helix configuration contains 3.6 peptide units per turn of the helix, so even the relatively small helix of not quite three turns shown in Figure 4(c) will have a dipole moment of about 34 D. Such a helix dipole moment is equivalent to there being half a positive electronic charge at the N-terminus and half a negative charge at the C-terminus. The electrostatic field associated with helix dipole moments can be expected to aid in the binding of ions to proteins. Also, dipole-dipole interactions between neighboring α-helical segments of the main polypeptide backbone should influence the overall protein conformation (38).

The effective dipole moment value for small globular proteins, obtained from measurements of the dielectric increment and the use of Equation (9), is typically of the order of several hundred Debye units. Examples of the dielectric dispersions exhibited by protein solutions are shown in Figure 5 for bovine serum albumin (BSA) and myoglobin. The fall in the relative permittivities from a value of around 90 to 70 arises from the rotational relaxation of the protein molecule and is referred to as the β-dispersion. BSA is a larger molecule than myoglobin and hence its relaxation time (c.f. Equation 8) is greater

than that for myoglobin. For frequencies below 10 KHz for BSA and below 1 MHz for myoglobin the rotational motion of the protein molecules can contribute fully to the polarizability of the solutions, and as the polarizability per unit volume for the proteins is greater than that of a water molecule, the resultant permittivity is greater than that of pure water. As the frequency is raised above the rate at which the protein molecules can rotationally reorientate, the protein molecules effectively act as polarizable "dead space", and the permittivity drops below the value of around 80 expected for bulk water. In evaluating the dielectric dispersion strength $\Delta\varepsilon$ to be used in Equation (9), this dielectric decrement should be added to the dielectric increment defined in Equation (10). Because the dielectric dispersion for glycine overlaps with that of water, the magnitude of this dielectric decrement is difficult to estimate for glycine solutions. Consequently, it was not included in the derivation of the correlation parameter g in the last section. However, the dielectric decrement for amino acids can be expected to be relatively small and so the underestimation in g will also be relatively small.

Careful examination by Essex et al. (39) of their results obtained for BSA revealed two components of the relaxation process, arising from the fact that the BSA molecule takes the form of a spheroid of axial ratio 1:3 and is capable of rotation about both its major axes. Essex et al. (39) were able to determine that the small fall in permittivity (the so-called $\delta$-dispersion) in the frequency range from around 10 MHz to 200 MHz could also be resolved into two separate processes. The process occurring at the higher frequency range was concluded to arise from relaxations of water molecules bound to the protein molecules. In Figure 5 the $\delta$-dispersion can also be clearly seen at a frequency of around 100 MHz for myoglobin. Although no firm conclusions could be made, the effect of fluctuating proton locations on the protein surface, and the relaxation of amino-acid side chains in the protein structure were considered to be the two most probable contributions to the other component of the $\delta$-dispersion for BSA. Other processes have also been considered to influence the dielectric properties of protein solutions, including the effect of the relaxation of the diffuse double layer formed around the protein molecule, and conduction processes associated with the movement of ions bound to the protein. Such effects have been described in detail elsewhere (26, 27) but in general they are considered to contribute little to the dielectric properties of protein solutions. Finally, the dispersion centered around 20 GHz for both the BSA and myoglobin solutions is due to the relaxation of water molecules which are not strongly associated with the protein molecules.

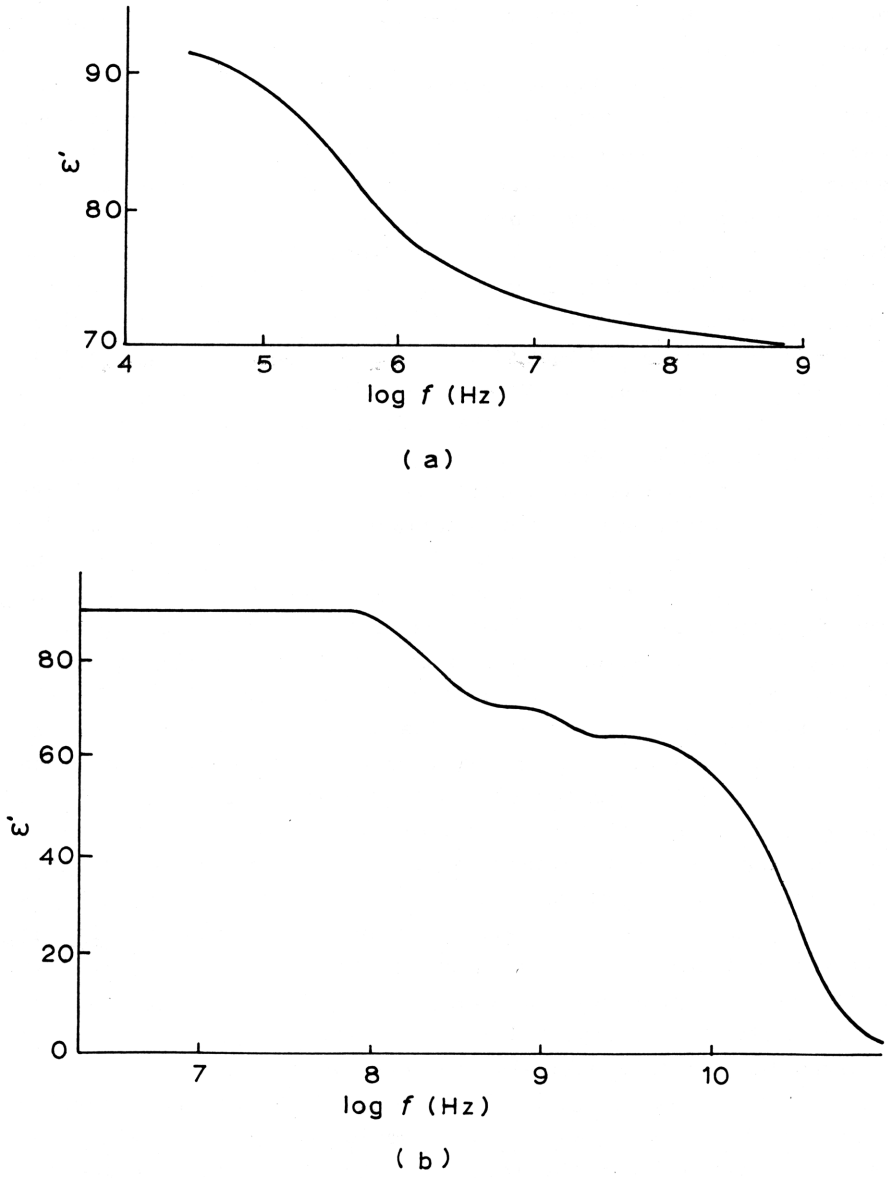


**Figure 5.** (a) The dielectric dispersion for a 100.8 mg/ml solution of bovine serum albumin (derived from reference (39)). (b) The dielectric dispersion for a 10% solution of myoglobin (from reference (26)).

It is generally found to be the case that the relaxation times for proteins, as derived from Equation (8), lead to molecular radii that are larger than the values which can be obtained directly from X-ray diffraction studies. The accepted way of interpreting this is to assume that there is a layer or two of water molecules (the so-called hydration sheath) so strongly associated or bound to the protein molecules, that they remain attached to the protein as it rotates. Water molecules that experience strong interactions with the protein structure can be expected to exhibit different relaxation processes compared to normal bulk water. There is supporting evidence to indicate that the $\delta$-dispersions described above are associated with relaxations of such protein-associated water molecules. We

shall return to this when considering the dielectric properties of protein-associated water.

## DNA

DNA, the molecule that contains the genetic library of living systems, is composed of two counter-opposed alpha-helical chains of polynucleic acids and can take the form of linear rods or supercoiled rings. These macromolecules can have molecular weights of $10^6$–$10^9$. Since the two helical chains point in opposite directions, the dipole moments of each chain cancel one another and this dipolar antiparallelism contributes towards the energy stabilization of the double helix structure. Althoughthe DNA macromolecule has no net helix-contributed dipole moment, early dielectric measurements (40-42) provided conclusive evidence for DNA molecules possessing large dipole moments directed along the axis of the double helix. This dipole moment arises from the fact that the DNA molecule is predominantly negatively charged when in aqueous solution, so that it will be surrounded by an atmosphere of counter-cations. Under the influence of an applied electric field these counter-ions will tend to be displaced along the surface of the DNA macromolecule and so give rise to a large induced dipole moment. The resulting dielectric dispersion will depend on the effective mobility of the ions along the macromolecule surface, and for rod-shaped macromolecules the relaxation time will be given by:

$$\tau = \pi\varepsilon L^2 / 2uzq^2$$

where $\varepsilon$ is the effective permittivity of the surrounding ionic atmosphere of $z$ ions per unit length, $u$ is the counter-ion surface mobility and $L$ is the length of the DNA macromolecule. Such an $L^2$ dependence for the dielectric relaxation time has been observed (43). The dielectric relaxation times are commonly found to be of the order 1 msec and dielectric dispersion strengths $\Delta\varepsilon$ are large and usually greater than 1000.

Apart from dielectric dispersions arising from the induced dipole moment associated with the electrical double layer around the macromolecule, a smaller dispersion occurs between 1–50 MHz (44, 45). The variation of the relative permittivity of an aqueous1% DNA solution is shown in Figure 6 for the range from 200 KHz to 10 GHz. The high-frequency tail of the induced dipolar dispersion is clearly evident, as is the dispersion around 20 MHz which is considered to arise from polar groups in the DNA molecule (45). The high-frequency dispersion arises from the relaxation of the unbound solvent water molecules and does not differ markedly from normal bulk water.

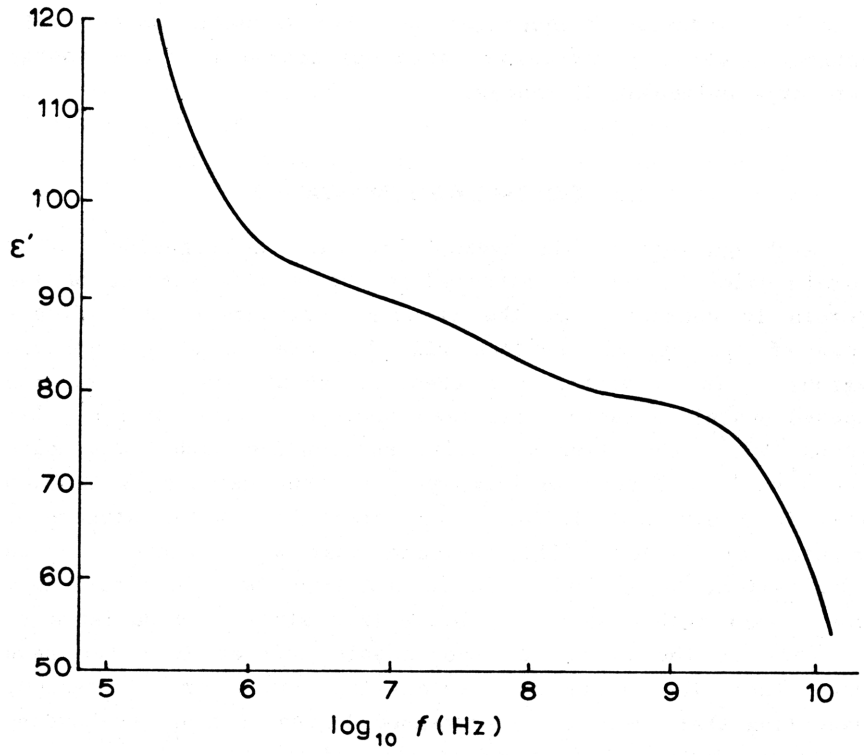


**Figure 6.** The dielectric dispersion from a 1% aqueous DNA solution (from reference (45)).

These observations by Takashima et al. (45) that the dielectric absorption of an aqueous solution of DNA does not differ appreciably from normal bulk water at l–10 GHz is of great interest in view of reports of large resonance absorptions in DNA solutions at these frequencies. Swicord and Davis (46, 47) and Edwards et al. (48, 49) have provided detailed evidence for the possibility that aqueous solutions of DNA molecules at room temperature can resonantly absorb microwave energy, and that the mechanism for this is associated with the coupling of the electric field to acoustic modes in the macro-molecular structure. If such resonance effects can be confirmed they will have significant implications, such as the possibility that biochemical processes could be influenced by highly selective microwave frequencies and that acoustic modes could possibly provide a mechanism for transporting coherent energy over large molecular distances.

## BIOLOGICALLY BOUND WATER

Although most of the hydrophilic amino-acid residues of a protein molecule will be situated on the outside surface of the protein in contact with the aqueous environment, significant areas of the protein surface will be made up of hydrophobic regions. In lysozyme, for example, about one half of the exposed protein structure has been found to consist of non-polar groups (50). The water molecules surrounding such hydrophobic

groups will be forced to form hydrogen-bond networks with each other in a way that differs from normal bulk water structure. Computer simulations (51) indicate that such water-structure modifications can extend at least 10Å into the bulk liquid away from a hydrophobic surface. Dielectric studies by Hallenga et al. (52) of the effect of hydrophobic solutes in water have shown that the dielectric relaxation times are increased, suggesting that there is an increased degree of hydrogen-bonding in the immediate neighborhood of the hydrophobic solutes. Some water molecules will form hydrogen bonds with the protein structure, and others will experience strong electrostatic interactions with charged groups such as glutamic acid and lysine. Water molecules near charged membrane surfaces will be similarly affected. All of these factors lead to the concept of there being a layer or two of water molecules near biomacromolecular surfaces having differing physical and dielectric properties from normal bulk water.

The existence of protein-associated or bound water in biological systems which as a result of its having hindered rotational mobility exhibits dielectric properties that differ from normal bulk water was first indicated by studies of the dielectric properties of protein solutions at microwave frequencies (53). On extrapolating the results to frequencies below where relaxation for normal water occurs, it was found that the relative permittivity value was lower than that for normal bulk water. This difference was assumed to be mainly due to the existence of water "irrotationally" bound to the protein molecules. Depending on the molecular shape assumed for the protein, the amount of such bound water was calculated to be 0.2–0.4 wt% of the protein. The identification of the $\delta$-dispersion in terms of such bound water was first described by Schwan (19) and Grant (18) in studies of hemoglobin and albumin solutions.

By making measurements of the dielectric properties of hydrated protein powders, effects associated with rotations of the protein molecules and relaxations of electrical double layers are avoided. This enables the dielectric properties of the protein-bound water to be investigated directly. Measurements by Bone et al. (54, 55) of the microwave dielectric properties of protein powders as a function of hydration indicate that 7–8% of the water molecules associated with a fully hydrated protein are bound, and are unable to contribute to the dielectric properties at 10 GHz. This is within the frequency range at which normal bulk water exhibits a strong dielectric absorption. Later investigations (56) of the $\delta$-dispersion for hydrated lysozyme powders indicate that about 36 water molecules are tightly incorporated into each lysozyme molecule and form an integral part of the overall protein structure. It was also concluded that vibrational motions of the protein structure contribute to the overall $\delta$-dispersion, especially at the higher hydration levels where the water appears to act as a plasticizing agent for protein structures (57).

The physical state of water associated with DNA molecules has also been investigated dielectrically. Microwave studies (58) on herring sperm DNA at 90–300°K have shown that a considerable proportion of the bound water, corresponding to around

280 water molecules per DNA helix turn, exhibit significantly different properties from those of normal bulk water in terms of dielectric relaxations below 273°K. An effective freezing point depression of 138°K was observed, indicating that a lose of rotational mobility of the DNA-associated water molecules with decreasing temperature is a much more gradual process than occurs in the normal water–ice transition. The collective nature of the interactions that can exist between water molecules and DNA has been clearly demonstrated by the computer simulations of Clementi (59) who showed that for hydrations up to around 270 water molecules per DNA helix turn the ensemble of water molecules is structured so as to reproduce a global image of the DNA electric field.

The presence of fluctuating proton populations will be of relevance to the dielectric properties of structural and membrane-bound proteins, and also of possible significance concerning proton conduction pathways. In an important series of measurements (60), significant details were obtained of the protein–water interactions for lysozyme. Measurements of the optical absorbance at 1580 $cm^{-1}$ (which was earlier mentioned as the characteristic absorbance of the CO $O^-$ carboxylate ion) and the specific heat as a function of hydration, indicated that the first water molecules to bind to lysozyme interacted with the ionizable carboxylic and basic groups. At around 5 wt% redistribution of the proton population appeared to occur, together with transitions in the protein–water and water–water hydrogen-bonding networks. Proton transport effects as a function of hydration for protein powders have been described by Gascoyne et al. (61) and Behi et a1. (62) and these measurements indicate that protons are able to migrate relatively freely in protein structures. Cyclodextrins have found use as artificial enzymes, and studies by Bone and Pethig (22) have shown that the flip-flop hydrogen bond networks that occur in the cyclodextrin hydrates provide a useful model system for studying proton conductivity.

## BIOLOGICAL ELECTROLYTES

Mammals have a total body water content of around 65 to 70%, and apart from the effects of dissolved biomacromolecules and membrane surfaces, the dielectric properties of this water are influenced by dissolved ionic salts. The physical effects of such dissolved ions on the dielectric permittivity of biological fluids arise from more than simple the volume effect of replacing polar water molecules by non-polar ionic particles. The strong local electric field around each dissolved ion has the effect of orientating the water molecules, thereby reducing the way they can rotate in response to an applied electric field. In the case of amino acids in solution, an equation of the form of Equation (10) can be used to describe the permittivity $(\varepsilon)$ of dilute electrolytes and that $(\varepsilon_1)$ of the pure aqueous solvent in terms of a dielectric decrement as follows:

$$\varepsilon = \varepsilon_1 - \delta c$$

where $\delta$ is the sum of the decrements arising from the cation and anion and is given by:

$$\delta = \left(\delta^+ + \delta^-\right).$$

Values of $\delta^+$ and $\delta^-$ for various ions in water are given in Table 1 for concentrations, $c$, of less than 1 molar. To estimate the extent to which, for example, KCl will reduce the permittivity of water, then from Table 1 the total decrement value for $K^+$ plus $Cl^-$ is $\delta = 11$, giving the room temperature relative permittivity for aqueous molar KCl solution as $\varepsilon = 68$ (for pure water, $\varepsilon_1 = 79$).

**Table l.** Dielectric Increment Values for Some Ions In Aqueous Solution

| CATION | $\delta^+$ (±1) | ANION | $\delta^-$ (±1) |
|---|---|---|---|
| $Na^+$ | 8 | $Cl^-$ | 3 |
| $K^+$ | 8 | $F^-$ | 5 |
| $Li^+$ | 11 | $I^-$ | 7 |
| $H^+$ | 17 | $SO^{2-}$ | 7 |
| $Mg^{2+}$ | 24 | $OH^-$ | 13 |

Besides lowering the relative permittivity of the aqueous solvent, dissolved ions generally increase the relaxation frequency. One exception to this is the effect of protons in decreasing the relaxation frequency. To a first approximation this effect can be considered to result from the solvated ions disrupting the hydrogen bond structure of normal water. For concentrations of less than 1 molar this effect can be expressed in terms of a relaxation frequency increment by the equation

$$f = f_1 + c\delta f$$

where

$$\delta f = \left(\delta f^+ + \delta f^-\right)$$

represents the effect of the cation and anion. Values for $f^+$ and $f^-$ are given in Table 2 and can be used to estimate how far the relaxation frequencies for various electrolytes differ from the value of 17.1 GHz for pure water at 20°C.

**Table 2.** Relaxation Frequency Increment Values for some Ions in Aqueous Solution

| CATION | $\Delta F^+$ (±0.2) GHz | ANION | $\Delta F^-$ (±0.2) GHz |
|---|---|---|---|
| $H^+$ | -0.34 | $OH^-$ | 0.24 |
| $Li^+$ | 0.34 | $Cl^-$ | 0.44 |
| $Na^+$ | 0.44 | $F^-$ | 0.44 |
| $K^+$ | 0.44 | $SO^{2-}$ | 1.20 |
| $Mg^{2+}$ | 0.44 | $I^-$ | 1.65 |

The overall AC conductivity of a biological material is given by

$$\sigma(f) = \sigma_0 + 2f\varepsilon_0\varepsilon''$$

where $\sigma_0$ is the conductivity arising from electric-field induced motions of the various ions in the electrolyte, and has the value:

$$\sigma_0 = q\sum_i z_1 n_i u_i \tag{11}$$

In this equation, $i$ denotes an ion species with valency $z$, concentration $n$ and electrical mobility $u_i$. The mobility values for some biologically relevant cations and anions are listed in Table 3. A pH of 7.0 at 24°C is equivalent to there being $10^{-7}$ moles of $H^+$ and $OH^-$ ions in a liter of water. This corresponds to a concentration of $6.03 \times 10^{19}/m^3$ of $H^+$ and $OH^-$ ions. The conductivity of pure water at 24°C can then be calculated from Equation (11), using mobility values for $H^+$ and $OH^-$ given in Table 3, as $5.4 \times 10^{-6}$ mho/m. In fact, $H^+$ ions as such do not exist to a significant extent in aqueous solution since they rapidly become hydrated to the $H_3O^+$ ion. The mobility of the $H_3O^+$ ion (Table 3) is the same as that of the proton. This is because the apparent mobility of the hydronium ion is equal to the rate at which protons transfer between neighboring hydrogen-bonded water molecules. The positive charge can move a considerable distance (creating a hydronium ion whenever it resides on a water molecule) with little movement of the water molecule themselves.

**Table 3.** The Electrical Mobility of Some Ions in Dilute Aqueous Solution at 25°C

| CATION | MOBILITY ($10^{-4}$ $cm^2$/V.sec) | ANION | MOBILITY ($10^{-4}$ $cm^2$/V.sec) |
|---|---|---|---|
| $Na^+$ | 8 | $Cl^-$ | 3 |
| $K^+$ | 8 | $F^-$ | 5 |
| $Li^+$ | 11 | $I^-$ | 7 |
| $H^+$ | 17 | $SO^{2-}$ | 7 |
| $Mg^{2+}$ | 24 | $OH^-$ | 13 |

It is often more convenient to deal with the effective molar conductivities of ions, and these values are given in Table 4 for dilute solutions. The conductivity of a dilute electrolyte can then be found from the equation:

$$\sigma = \sum_i m_i \sigma_{mi} \tag{12}$$

where $m_i$ is the molar concentration of ion species $i$ having a molar conductivity$\sigma mi$. The most dominant ions in human tissue fluids are those of sodium and chlorine, each of concentration around 150 mM per liter, which is equivalent to a 0.9 wt% saline solution. From Table 4 and Equation (12) the conductivity of such a solution at 25°C can be calculated to be 1.83 mho/m. The average water content of various tissues is listed in Table 5. For liver and muscle the water content is about 75%. To a first approximation

**Table 4.** Molar Conductivity of Some Ions in Dilute Aqueous Solution at 25°C

| CATION | CONDUCTIVITY (mho.cm$^2$/mol) | ANION | CONDUCTIVITY (mho.cm$^2$/mol) |
|---|---|---|---|
| $H^+$, $H_3O^+$ | 350 | $OH^-$ | 193 |
| $K^+$ | 73 | $Cl^-$, $I^-$ | 74 |
| $Na^+$ | 48 | $F^-$ | 52 |
| $NH^{4+}$ | 73 | $Br^-$ | 75 |
| $Ca^{2+}$ | 119 | $SO^2{}_4{}^-$ | 160 |

then, the conductivity should be around 1.4 mho/m. As described later in this Chapter (see Table 7) this accurately predicts the conductivity at frequencies around 1 GHz, where the electrical properties of tissues are determined by the electrolyte content and not by the tissue structures themselves, and before frequencies are attained where the dielectric relaxation of water molecules becomes the dominant effect.

**Table 5.** Water Content Values for Various Tissues and Organs

| TISSUE | WEIGHT % WATER CONTENT | TISSUE | WEIGHT % WATER CONTENT |
|---|---|---|---|
| Bone | 44–45 | Lung | 80–83 |
| Bone Marrow | 8–16 | Muscle | 73–78 |
| Bowel | 60–82 | Ocular Tissues | |
| Brain | | Choroid | 78 |
| White matter | 68–73 | Cornea | 75 |
| Grey matter | 82–85 | Iris | 77 |
| Fat | 5–20 | Lens | 65 |
| Kidney | 78–79 | Retina | 89 |
| Liver | 73–77 | Skin | 60–76 |
| | | Spleen | 76–81 |

## MEMBRANES AND CELLS

As we have already discussed, cell membranes are ultrathin structures of thickness around 6 nm. They are composed mainly of long-chain hydrocarbon (lipid) molecules and proteins. The relative permittivity of a close packed assembly of lipids and proteins, such as exists in membrane structures, can be expected to be of the order 3. An approximate value for the effective capacitance per unit area of such a membrane can be found using the basic equation:

$$C = \varepsilon_0 \varepsilon / d$$

Assuming a thickness $d$ of around 6 nm and a relative permittivity $\varepsilon$ of 3.0, then the membrane capacitance can be estimated to be 0.44 $\mu F/cm^2$, which compares favorably with the range 0.5–1.3 $\mu F/cm^2$ commonly observed for a wide range of biological membranes (63). Although cell membranes are largely hydrophobic, it is known that some water molecules are incorporated into membrane structures. Their presence, together with the possibility that the membrane-associated proteins can exhibit some degree of lateral diffusion and rotational freedom, will increase the effective overall polarizability of the membrane and increase the capacitance value estimated above to be within the observed range of values. Being largely composed of hydrocarbon-based lipid and protein molecules, the electrical resistivity of cell membranes can be expected to be large.

The capacitive and resistive components of a cell membrane can be represented as an equivalent electrical circuit of the form of Figure 7(a), where the membrane capacitance $C_m$ is shown in parallel with the membrane resistance $R_m$. A feature of this circuit is that with increasing frequency the resistance $R_m$ is increasingly short-circuited by the

reactance $\left(1/\omega C_m\right)$of $C_m$. The consequence of this as far as the electrical properties of a cell in aqueous suspension is concerned is shown schematically in Figure 8. At low frequencies (Figure 8a) the resistance of the cell membrane insulates the cell interior

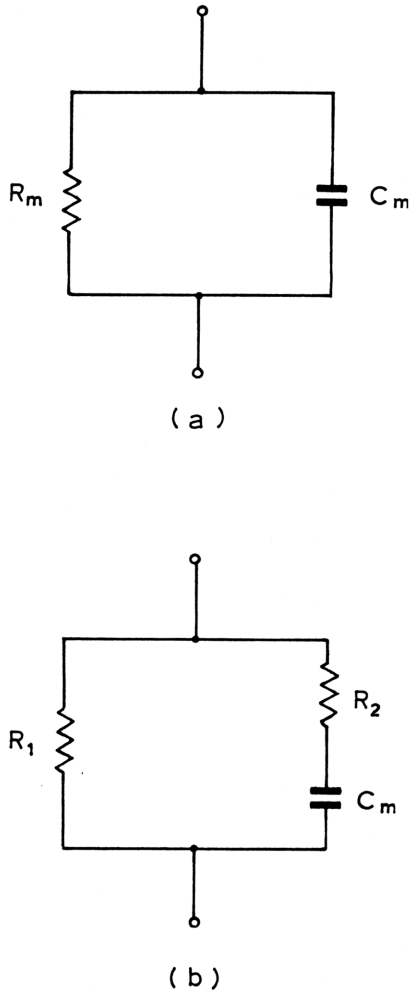


**Figure 7.** (a) Equivalent electrical circuit for a cell membrane, where $C_m$ and $R_m$ are the membrane capacitance and resistance, respectively. (b) An equivalent circuit for a cell, where $R_1$ is the resistance of the extracellular electrolyte, $C_m$ is the membrane capacitance, and $R_2$ is a function of the membrane and cytoplasm resistance.

(cytoplasm) from an external electric field, and no electrical current is induced within the cell interior. In dielectric terms, the cell appears to take the form of an insulating spheroid, and it increases the effective resistivity of the aqueous suspension. At higher frequencies (Figure 8b) the short-circuiting effect of the membrane capacitance allows

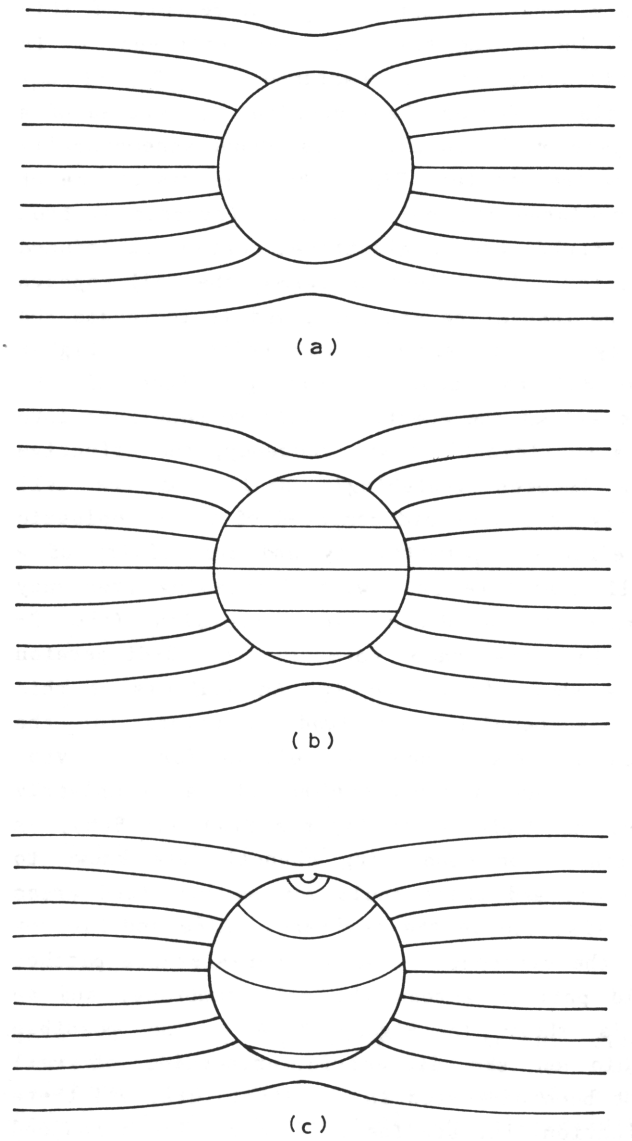


**Figure 8.** (a) At low frequencies the membrane resistance shields the cell interior from applied electric fields. (b) At higher frequencies the membrane resistance is progressively shorted-out by the membrane capacitance. (c) The effect of a conducting pore in the membrane is to change the voltage stress across the membrane compared to the commonly accepted picture of (a) above. (From reference (64)).

the electric field to penetrate into the cell until, at a sufficiently high frequency, the effective membrane resistance becomes vanishingly small and the cell appears dielectrically as a spheroid composed of the cytoplasmic electrolyte. The effective permittivity and resistivity of a cell suspension will therefore fall with increasing frequency and this gives rise to a dielectric dispersion (the ß-dispersion) of roughly the same form as the ß-dispersion exhibited by tissues shown in Figure 9. An analysis of this dispersion for cell suspensions can lead to values for the membrane capacitance and

resistance, as well as for the cytoplasm resistivity. The representation of a completely insulating membrane, as depicted in Figures 8(a) and 8(b), is only an approximation. Ion conducting channels are known to exist in cell membranes and these could act as localized areas of relatively low resistance in the membrane. Klee and Plonsey (64) have shown how the existence of such low-resistance patches can alter the field pattern across the cell membrane, and an example of this is shown in Figure 8(c). The possible consequences of this on the dielectric properties of cell suspensions have not been addressed in the literature, and there could also be implications for studies of electric field induced cell-to-cell fusions (65).

An equivalent electrical circuit that is often used to represent a cell is shown in Figure 7(b), where $R_1$ represents the resistance of the extracellular medium, $C_r$ is the membrane capacitance and $R_2$ is a function of both the membrane resistance and cytoplasm resistance. A full discussion of the analysis of the equivalent electrical circuits for cells and biological tissues is given by Schanne and Ceretti (31). These authors, together with Cole (30), also provide a comprehensive account of the values that have been obtained for the electrical properties of a variety of cell and bacterial membranes and cytoplasms. Values for cell membrane resistance of $10^3$–$10^5$ ohm cm$^2$ and cytoplasm resistivity of 0.3–7 ohm/n have been obtained.

Cell membranes contain ionizable acidic and basic groups, although for most cells so far studied the acidic groups are dominant and the membranes carry a net negative charge. At the immediate interface between a cell membrane and its aqueous environment there will therefore be an electrical double layer formed by the charged groups on the membrane and the counter-ions in the electrolyte, as depicted in Figure 1(a). As for the case of DNA, we shall expect to find for cell suspensions a dielectric dispersion associated with ionic surface conduction effects and relaxations of the double layer, and in fact such a dispersion is found (the $\alpha$-dispersion) of the same form as the $\alpha$-dispersion shown in Figure 9. Similar dispersions can be observed for colloidal suspensions of glass or polystyrene spheres in electrolytes and also as a result of electrical polarizations at electrode-electrolyte interfaces. Recent studies (20, 66) of the dielectric properties of bacterial suspensions have provided convincing evidence that effects associated with the diffusional motions of lipids and proteins in the membranes also contribute to the $\alpha$-dispersion. Field induced diffusions of membrane proteins have been observed microscopically (67), and such effects are relevant to possible physiological effects of electrical fields.

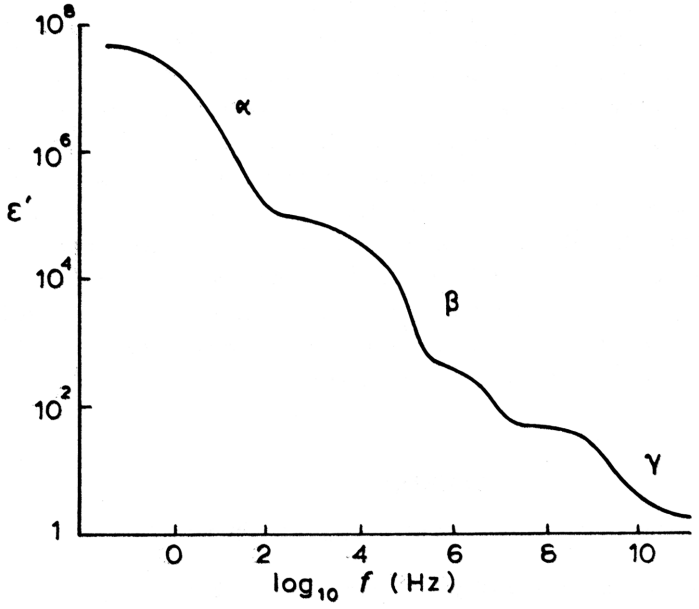


**Figure 9.** An idealized representation of the way in which the relative permittivity of a typical biological tissue varies with frequency.

## TISSUES

### FREQUENCY DEPENDENCE OF DIELECTRIC PROPERTIES

The relative permittivity of biological tissue typically decreases with increasing frequency in three major steps which are designated as the α-, ß-, and γ-dispersion, and an idealized representation of this is shown in Figure 9. The α-dispersion is generally considered to be associated with interfacial polarizations associated with electrical double layers and surface ionic conduction effects at membrane boundaries. The ß-dispersion in Figure 9 is shown to have two components and, although such fine detail is not commonly found in reality, the purpose of representing it in this way is to indicate that both capacitive shorting-out of membrane resistances and rotational relaxations of biomacromolecules can contribute to this dispersion. The γ-dispersion arises from the relaxation of free water in the tissue.

Comparatively little work has been reported for the dielectric properties of tissue in the frequency range up to a few KHz, but a good example of the α-dispersion has been obtained by Singh et al. (68) for *in vitro* measurements on freshly excised kidney and *in vivo* measurements using external electrodes for normal breasts and breasts with malignant tumors. Some of these results are shown in Figure 10 and it can be seen that malignancy appears to influence the observed dielectric properties. The possible cause for

the difference in the dielectric properties of normal and cancerous tissue will be discussed later in this Chapter. Another good example of the α-dispersion can be found in the results of Kosterich et al. (69) for freshly excised rat femurs, where the permittivity was observed to fall from $10^4$ at 10 Hz to around 100 at 1 MHz. In the early work by Schwan (70), the α-dispersion was clearly demonstrated for muscle tissue and an important aspect of this work was the observation that the permittivity and resistivity measured at 1 KHz decreased steadily with time after excision of the tissue. This effect is consistent with the steady loss of integrity and physiological viability of the cell membranes.

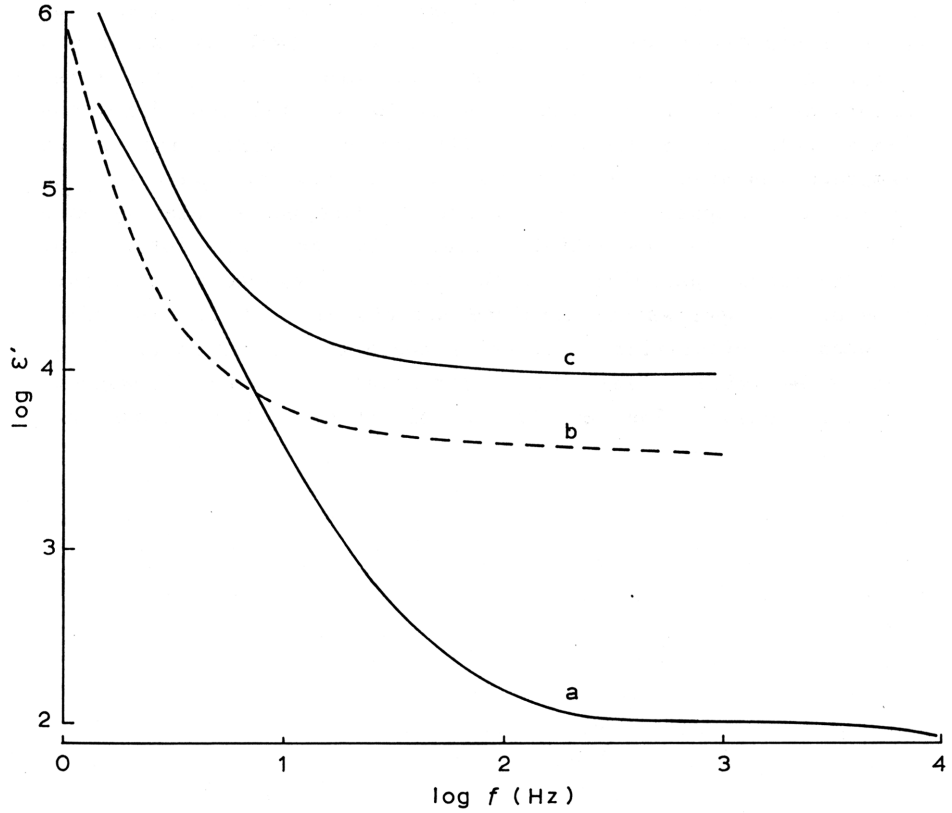


**Figure 10.** Frequency variation of the relative permittivity of (a) human kidney, (b) normal breast and (c) breast with malignant tumor (from reference (66)).

The dependence of the ß-dispersion upon the integrity of cell membranes was clearly shown (Figure 11) by Pauly and Schwan (71), who measured the effect of digitonin in lysing the fiber membranes of bovine eye lens. Until now we have considered the ß-dispersion to be associated with the short-circuiting of the membrane resistance by the membrane capacitance. Whereas this is now the accepted interpretation, it does not completely make clear that the essential effect is one of interfacial polarizations associated with the heterogeneous structure inherent in membrane-electrolyte structures. At the interface between two dissimilar dielectrics there is a build-up of charge and this gives rise to interfacial, or Maxwell-Wagner, polarizations. The magnitudes of these polarizations are dependent on the conductivity, permittivity and geometry of the separate

components of the heterogeneous structure. With increasing frequency, the more resistive components are neutralized by their associated parallel capacitances. The structure therefore becomes progressively more (electrically) homogeneous. A full account of the theories of interfacial polarizations of relevance to biological materials has been given elsewhere (27).

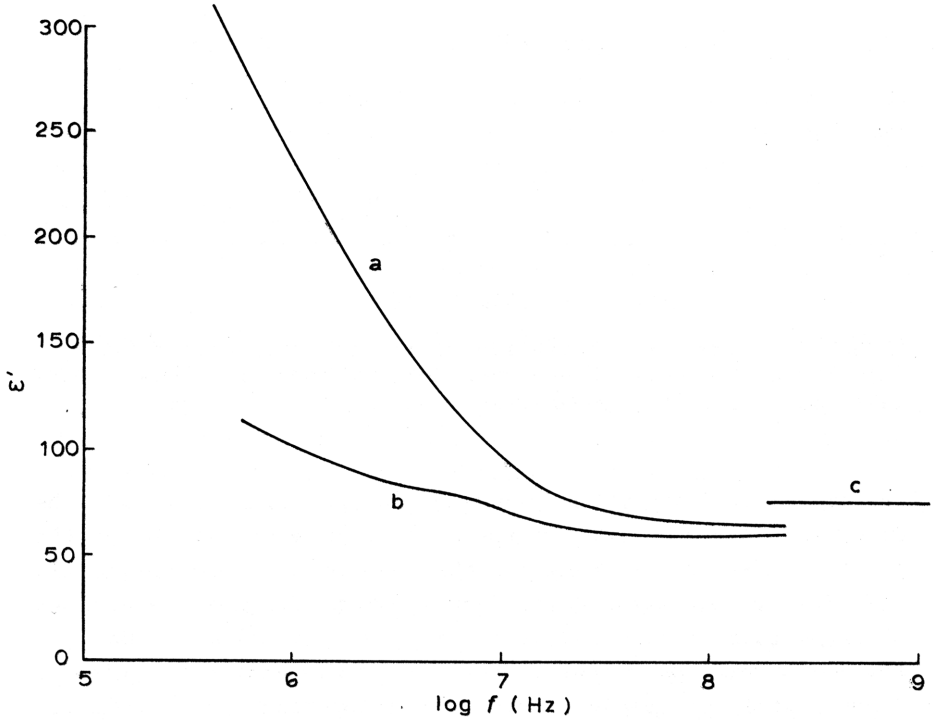


**Figure 11.** (a) Frequency variation of the relative permittivity of bovine eye lens fiber suspension and (b) the effect of digitonin lysis of the fiber membrane (71). (c) Permittivity of 0.9% NaCl solution at 27°C.

Also shown in Figure 11 is the permittivity of 0.9% sodium chloride solution, which corresponds to the ionic strength of cellular fluid. It can be seen that above 100 MHz the dielectric properties of tissue become largely independent of the membrane structures. The permittivity of tissue in the region 100 MHz to 1 GHz is a little less than that of a 100% concentration of the aqueous cellular fluids due to the presence of the non-polar membrane materials and other chemicals of low polarizability.

For frequencies higher than about 100 MHz, where the capacitive shorting-out effects of the cell membrane resistances begins to take effect, the dielectric characteristics of tissues can be expected to reflect the properties of the inter- and intra-cellular electrolytes and, in particular, to exhibit a dielectric dispersion associated with the relaxation of water dipoles. This can be seen in Figure 12, where the relative permittivity and resistivity values of brain, fat and muscle above 100 MHz are shown alongside those exhibited by 0.9% saline solution. Resistivity values, rather than conductivity, are used in Figure 12 as this aids in showing the differences in the electrical properties at the higher

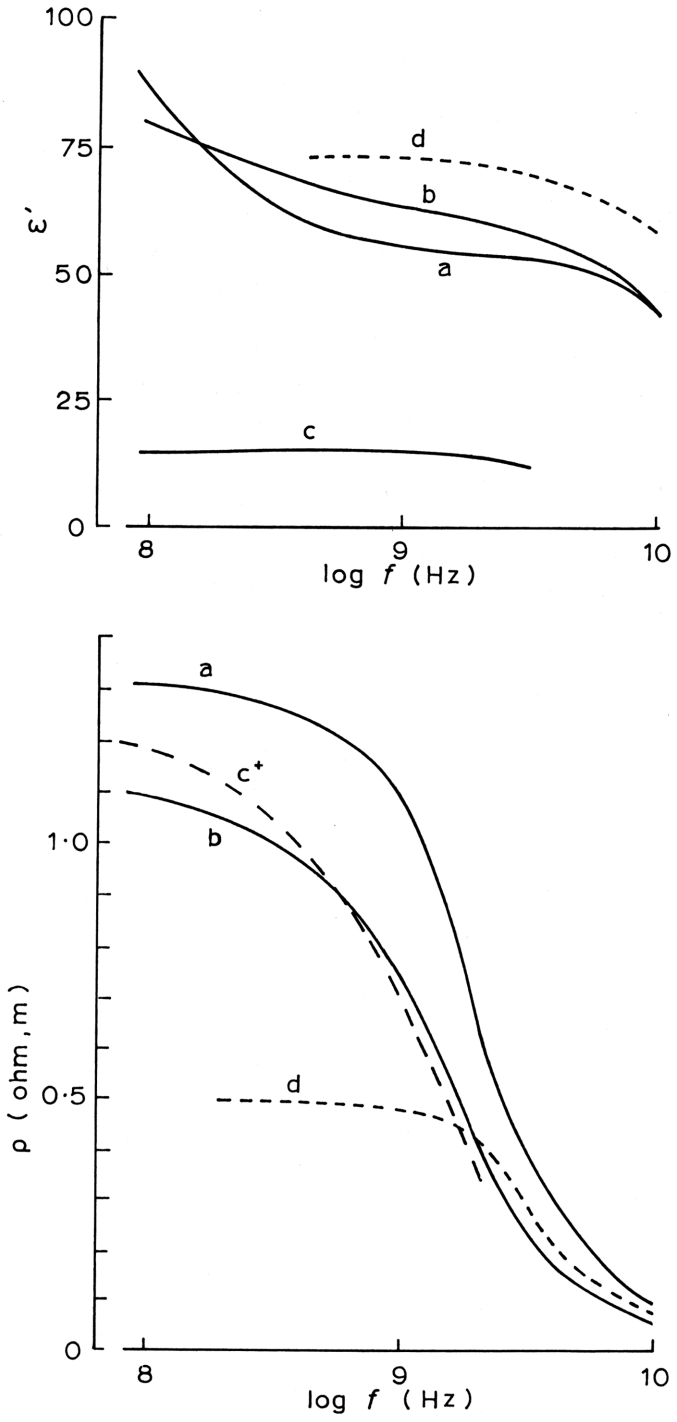


**Figure 12.** *In vivo* permittivity and resistivity measurements obtained (101) for (a) rat brain, (b) rat muscle and (c) rat fat (scaled down by one-fifth). (d) 0.9% saline solution.

frequencies. A feature that can also be deduced from this figure is that the dielectric

properties of tissues are influenced by their tissue water content. Muscle, for example, which in man can have water contents of 73–77.6 wt%, exhibits a much larger permittivity and conductivity compared to those of fat whose water content is 5–20 wt%. The water contents of various tissues are given in Table 5. In their studies of liver, muscle and skin, Schwan and Foster (72) concluded that the microwave dielectric properties of these tissues could be attributed directly to their free water contents, and also to the dispersion expected for normal bulk water. A similar conclusion was obtained by Foster et al. (73) for the microwave dielectric properties of canine brain tissue. These studies show that for frequencies above 100 MHz the dielectric properties of tissue are consistent with those expected for a suspension of low conductivity, low permittivity, particles (cells) in an aqueous electrolyte.

## SKIN

The dielectric properties of skin are of relevance to a large number of therapeutic and diagnostic techniques which involve the application or monitoring of electrical signals. There is also interest within the cosmetics industry in using the dielectric properties of skin as an indicator of the efficacy of dermatological and cosmetic treatments. The electrical properties of skin are largely determined by the corneum which has a thickness of the order 15 μm and consists of layers of dead cells. As these dead cells, formed mainly of keratin and membrane material, are worn off from the skin surface they are replaced by underlying epidermal cells. The dielectric properties of skin show considerable regional variability over the body, with the impedance being lowest in areas such as the palms where sweat ducts are in abundance. Rosendal (74) measured the properties of wet, freshly excised, skin approximately 1 mm thick at 1 KHz and 10 KHz and obtained values for the effective capacitance and resistance of the corneum of 4.6 nF/cm$^2$ and 34.9 kΩ.cm$^2$, respectively. A value of 6.2 kΩ.cm$^2$ was obtained for the effective series resistance of the skin and underlying deep tissue. If the relative permittivity of dry keratinized membrane material is assumed to be around 10, then these results suggest that the capacitive–resistive element in skin has a thickness of the order 2 μm. This layer provides the protective barrier between the body tissues and the environment.

The average *in vivo* electrical properties of skin over the range 1 Hz to 1 MHz, determined by Yamamoto and Yamamoto (75), are shown in Figure 13(a). An understanding of these properties was approached in terms of the inhomogeneous structure and composition of skin, and the way in which this varies from the skin surface into the underlying dermis and subcutaneous tissue. The appearance of a relatively weak α-dispersion for skin should be noted, and this lack of a significant dispersion in the frequency range from around 10 Hz to 10 KHz could be associated with the dead nature of the corneum. Clar et al. (76) found that the dispersion exhibited by normal skin in the range of 0.5 Hz to 10 KHz was characterized by two separate relaxation processes,

centered around 80 Hz and 2 KHz, respectively. As a tentative proposal, the origin of these dispersions was considered to be located within the corneum and to be associated with relaxations of counterions surrounding the corneal cells. The dielectric response of psoriatic skin was found to differ significantly from that of normal skin. The dielectric properties determined by Schwan (19) for the microwave range of frequencies are shown in Figure 13(b), and from an interpolation of the two sets of results of Figure 9 the form of the ß-dispersion for skin can be estimated.

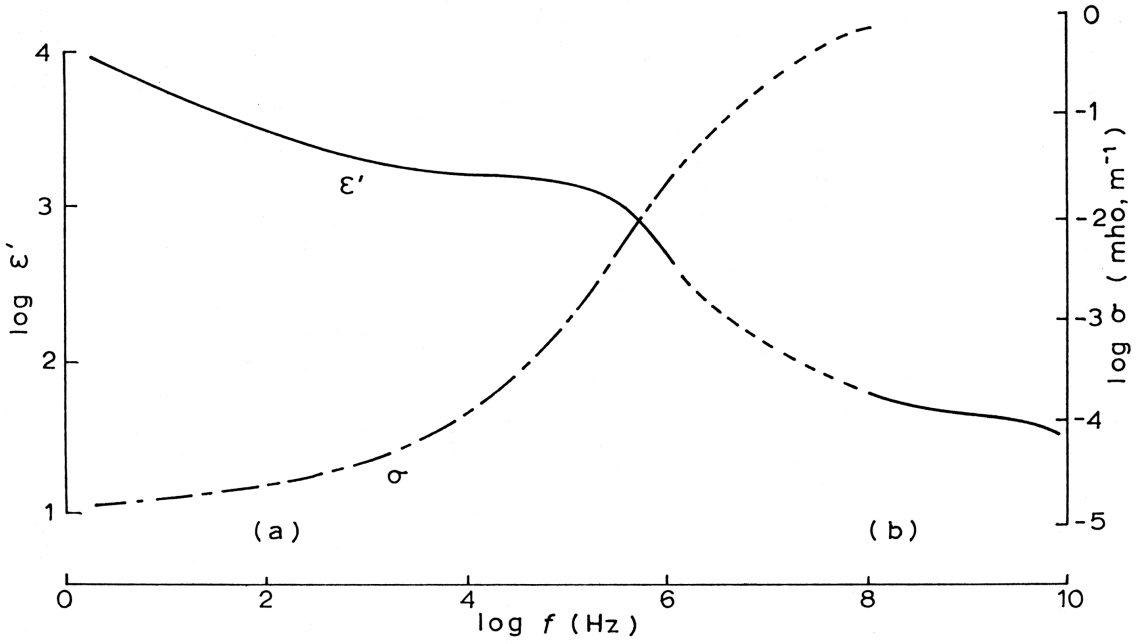


**Figure 13.** Frequency variation of the relative permittivity and conductivity for skin at 37°C (based on references (75) and (19)).

## OTHER TISSUES

The relative permittivity and conductivity of various tissues at 37°C are given in Tables 6 and 7, respectively, for several frequencies commonly used for therapeutic and diagnostic purposes. This data has been derived from the references cited, and although they represent the most reliable data presently available, they should be considered as representing average values. The tissue water contents given in Table 5 and the ranges for these can be used to estimate the likely spread of electrical properties expected for the various tissues. The data, mostly *in vivo*, was obtained for tissues of various animals (including man), but since the dielectric properties of the same tissue types from different animals are quite similar (77-79) this should not reduce the value of Tables 6 and 7.

**Table 6.** The Relative Permittivity of Biological Tissues at 37°C for Various Frequencies Commonly Used for Therapeutic Purposes

| MATERIAL | 13.56 MHz | 27.12 MHz | 433 MHz | 915 MHz | 2.45 GHz | REFERENCE |
|---|---|---|---|---|---|---|
| Artery | – | – | – | – | 43 | (80) |
| Blood | 155 | 110 | 66 | 62 | 60 | (81) |
| Bone | | | | | | |
| (with marrow) | 11 | 9 | 5.2 | 4.9 | .8 | (27) |
| in Hank's solution) | 28 | 24 | – | – | – | (70) |
| Bowel (plus contents) | 73 | 49 | – | – | – | (82) |
| Brain | | | | | | |
| (white matter) | 182 | 123 | 48 | 41 | 35.5 | (73) |
| (grey matter) | 310 | 186 | 57 | 50 | 43 | (73) |
| Fat | 38 | 22 | 15 | 15 | 12 | 104 |
| Kidney | 402 | 229 | 60 | 55 | 50 | 104, (78) |
| Liver | 288 | 182 | 48 | 46 | 44 | (78, 81) |
| Lung | | | | | | |
| (inflated) | 42 | 29 | – | – | – | (81, 82) |
| (deflated) | 94 | 57 | 35 | 33 | – | (81, 82) |
| Muscle | 152 | 112 | 57 | 55.4 | 49.6 | (83) |
| Ocular tissues | | | | | | |
| (choroid) | 240 | 144 | 60 | 55 | 52 | (84) |
| (cornea) | 132 | 100 | 55 | 51.5 | 49 | (84) |
| (iris) | 240 | 150 | 59 | 55 | 52 | (84) |
| (lens cortex) | 175 | 107 | 55 | 52 | 48 | (84) |
| (lens nucleus) | 50.5 | 48.5 | 31.5 | 30.8 | 26 | (84) |
| (retina) | 464 | 250 | 61 | 57 | 56 | (84) |
| Skin | 120 | 98 | 47 | 45 | 44 | (81), Fig. 13 |
| Spleen | 269 | 170 | – | – | – | (78) |

**Table 7.** The Conductivity (mho/m) of Biological Tissues at 37°C

| MATERIAL | 13.56 MHz | 27.12 MHz | 433 MHz | 915 MHz | 2.45 GHz | REFERENCE |
|---|---|---|---|---|---|---|
| Artery | – | – | – | – | 1.85 | (80) |
| Blood | 1.16 | 1.19 | 1.27 | 1.41 | 2.04 | (81) |
| Bone | | | | | | |
| (with marrow) | 0.03 | 0.04 | 0.11 | 0.15 | 0.21 | (78) |
| in Hank's solution) | 0.021 | 0.024 | – | – | – | (78) |
| Brain | | | | | | |
| (white matter) | 0.27 | 0.33 | 0.63 | 0.77 | 1.04 | (73) |
| (grey matter) | 0.40 | 0.45 | 0.83 | 1.0 | 1.43 | (73) |
| Fat | 0.21 | 0.21 | 0.26 | 0.35 | 0.82 | 104 |
| Kidney | 0.72 | 0.83 | 1.22 | 1.41 | 2.63 | 104, (78) |
| Liver | 0.49 | 0.58 | 0.89 | 1.06 | 1.79 | (81), (78) |
| Lung | | | | | | |
| (inflated) | 0.11 | 0.13 | – | – | – | (81), 100 |
| (deflated) | 0.29 | 0.32 | 0.71 | 0.78 | – | (81), 100 |
| Muscle | 0.74 | 0.76 | 1.12 | 1.45 | 2.56 | 102 |
| Ocular tissues | | | | | | |
| (choroid) | 0.97 | 1.0 | 1.32 | 1.40 | 2.30 | 80 |
| (cornea) | 1.55 | 1.57 | 1.73 | 1.90 | 2.50 | 80 |
| (iris) | 0.90 | 0.95 | 1.18 | 1.18 | 2.10 | 80 |
| (lens cortex) | 0.53 | 0.58 | 0.80 | 0.97 | 1.75 | 80 |
| (lens nucleus) | 0.13 | 0.15 | 0.29 | 0.50 | 1.40 | 80 |
| (retina) | 0.90 | 1.0 | 1.50 | 1.55 | 2.50 | 80 |
| Skin | 0.25 | 0.40 | 0.84 | 0.97 | – | (81), Fig. 13 |
| Spleen | 0.86 | 0.93 | – | – | – | (78) |

## TISSUE-BOUND WATER

The results of Figure 12 indicate that a large proportion of the water in tissues has rotational properties similar to those of normal bulk water. Schwan and Foster (72) obtained evidence to suggest that about l0% of the water in tissue is strongly bound and rotationally hindered, having a relaxation frequency 50–200 times lower than that for normal bulk water. A less pronounced lowering of the water relaxation frequency was observed by Gabriel et al. (84) for ocular tissues. The relaxation frequency of normal bulk water at 37°C is 25 GHz, whereas retina (89% water content) exhibited a relaxation frequency of around 2l GHz, and for the lens nucleus (65% water) this was reduced to

around 9 GHz. The lowering of the relaxation frequency with falling water content was an interesting feature of these studies. Stuchly et al. (79) obtained *in vivo* measurements of the dielectric properties of skeletal muscle, brain cortex, spleen and liver of live cats and rats for 0.1–10 GHz. Above 1 GHz the dielectric properties correlated well with the various tissue water contents, and it was deduced that practically all the water in skeletal muscle was in the form of bulk water. For the other tissues, both free and bound water were deduced to be present, with spleen having a total tissue water content (volume basis) composed of 69% free water and 9% bound water. For liver, the total water content (80%) was found to consist of 62% free water and 18% bound water. Relaxations of such bound water produce a relatively weak dielectric dispersion, called the δ-dispersion, centered around 100 MHz and hence is located roughly midway between the ß-and γ-dispersions. Most of the strongly bound water in tissues will be incorporated directly into the overall structure of the globular and membrane-associated proteins. It could be that perturbing the strongly bound water molecules by subjecting them to 100 MHz electromagnetic radiation induces changes in those physiological processes that depend on the functional behavior of the substrate proteins. such a possibility should be included by those who wish to consider the harmful effects that might arise from deliberate or accidental exposure to electromagnetic energy of 50–500 MHz.

## TUMOR TISSUE

The results shown in Figure 10 for breast cancer indicate that the permittivity of cancerous tissue is significantly greater than that of normal tissue. Such a trend was first noted by Fricke and Morse (85). This feature is also indicated by the data presented in Table 8, and is especially evident from the work of Bottomley and Andrew(86) for normal and cancerous rat liver, and from the measurements of Rogers et al. (87) on normal and tumor mouse muscle. The conductivity of cancerous tissue also appears to be greater than that of normal tissue, and this property, noted also by Foster and Schepps (88), could be of use in further developments of the radiofrequency and microwave hyperthermic treatment of cancer.

As summarized by Hazlewood et al. (89) the relaxation times in malignant tissue are larger than those in normal tissue, indicating that a significant increase in the motional freedom of water has occurred. The dielectric results may also relate to the observation that the water content and sodium concentration in tumor cells is higher than in normal cells (90, 91), and also to the facts that cancer cells have significantly reduced membrane potentials (92-94) and an altered ability to absorb positive ions (95, 96). By incorporating these known differences in the water and ionic compositions of normal and cancerous tissues, Grant and Spyrou (97) have successfully been able to model the interfacial polarizations to predict the dielectric differences that were observed by Bottomley and Andrew (86) for normal and cancerous rat liver.

**Table 8.** Relative Permittivity ($\varepsilon$) and Resistivity ($\rho$, ohm.m) Values for Some Tumor Tissues at 37°C

| MATERIAL | 13.56 MHz | | 27.12 MHz | | 433 MHz | | 915 MHz | | 2450 MHz | | REFERENCE |
|---|---|---|---|---|---|---|---|---|---|---|---|
| | $\varepsilon$ | $\rho$ | $\varepsilon$ | $\rho$ | $\varepsilon$ | $\rho$ | $\varepsilon$ | $\rho$ | $\varepsilon$ | $\rho$ | |
| Hemangiopericytoma | 136 | 0.91 | 106 | 0.88 | 57 | 0.73 | 55.4 | 0.62 | 50 | 0.35 | (83) |
| Intestinal Leiomysarcoma | 309 | 1.2 | 183 | 1.1 | 62 | 0.81 | 60 | 0.67 | 54 | 0.38 | (83) |
| Splenic Hematoma | 297 | 1.56 | 243 | 1.35 | 54 | 1.08 | 52 | 0.94 | 49 | 0.53 | (83) |
| Rat Hepatoma D23 | 305 | 1.35 | 178 | 1.15 | – | – | – | – | – | – | (86) |
| Normal Rat Liver | 167 | 2.05 | 110 | 1.90 | – | – | – | – | – | – | (86) |
| Canine Fibrosarcoma | 48 | 5.6 | 29 | 5.3 | (Before hyperthermia) | | | | | | (82) |
| | 30 | 1.55 | 19 | 1.51 | (After 4·C Hyperthermia) | | | | | | (82) |
| Mouse KHT Tumor | – | – | 135* | – | 61 | 0.89 | 60 | 0.62 | 54 | 0.39 | (87) |
| Normal muscle | – | – | 90* | | 56 | 1.08 | 56 | 0.66 | 48 | 0.38 | (87) |

It would also be of interest to investigate the possibility that the dielectric properties relate to the cellular electrochemical potentials. Tumor cells are more electronegative than normal cells (96), and cancerous tissues are more electronegative than normal tissues (98, 99). Such results suggest that structurally lese differentiated tissues are more electro-negative than normal tissues and it is of interest to note that regenerating tissue, which is another type of less differentiated tissue, is also relatively electronegative (100). Dielectric measurements may usefully complement such studies as those summarized here and provide new insights at the molecular level in the study of the cancer problem.

## REFERENCES

(1) Adey, W.R. and Lawrence, A.F. eds. Non-linear Electrodynamics of Biological Systems. Plenum Press, New York, 1984.

(2) Becker, R.O. and Marino, A.A.: Electromagnetism and Life. State University of New York Press, Albany, 1982.

(3) Fröhlich, H. and Kremer, F. eds. Coherent Excitations in Biological Systems. Springer-Verlag, Heidelberg, 1983.

(4) Konig, H.L., Drueger, A.P., Lane, S. and Sonnig, W.: Biological Effects of Environmental Electromagnetism. Springer-Verlag, Heidelberg, 1981.

(5) Sheppard, A.R. and Eisenbud, M. eds. Biological Effects of Electric and Magnetic Fields of Extremely Low Frequency. New York University Press, New York, 1977.

(6) Hahn, G.M.: Hyperthermia and Cancer. Plenum, New York, 1982.

(7) Storm, F.K. ed. Hyperthermia in Cancer Therapy. G.K. Hall, Boston, 1983.

(8) Baker, L.E. Electrical impedance pneumography. In: Rolfe, P. ed., Non-invasive Physioloigcal Measurements. Academic, London, 1979.

(9) Hill, D.W. The role of electrical impedance methods for the monitoring of central and peripheral blood flow changes. In: Rolfe, P. ed., Non-invasive Physiolgoical Measurements. Academic, London, 1979.

(10) Barber, D.C. and Brown, B.H.: Applied potential tomography. J. Phys. [E] 17: 723-733, 1984.

(11) Pryce, L.R.: Electrical impedance tomography (ICT): a new CT imaging technique. IEEE Trans. Nucl. Sci. NS-26: 2736-2739, 1979.

(12) Burdette, E.C., Wiggins, S., Brown, R. and Karow, A.M.: Microwave thawing of frozen kidneys: a theoretically based experimentally-effective design. Cryogiology 17: 393-402, 1980.

(13) Barker, A.T. and Lunt, M.J.: The effects of pulsed magnetic fields of the type used in the stimulation of bone fracture healing. Clin. Phys. Physiol. Meas. 4: 1-27, 1983.

(14) Höber, R.: Eine methode die elektrische leitfahigkeit im innern von zellen zu messen. Arch. Gesamt. Physiol. Mensch. 133: 237-259, 1910.

(15) Fricke, H.: The electric capacity of suspensions with special reference to blood. J. Gen. Physiol. 9: 137-152, 1925.

(16) Oncley, J.L. The electrical moments and relaxation times of proteins as measured from their influence on the dielectric constant of solutions. In: Cohen, E.J. and Edsall, J.T. eds., Proteins, Amino Acids and Peptides. Reinhold, New York, 1943.

(17) Haggis, G.H., Buchanan, T.J. and Hasted, J.B.: Estimation of protein hydration by dielectric measurements at microwave frequencies. Nature 167: 607-608, 1951.

(18) Grant, E.H.: The structure of water neighboring proteins, peptides, and amino acids as deduced from dielectric measurements. Ann. N.Y. Acad. Sci. 125: 418-427, 1965.

(19) Schwan, H.P.: Electrical properties of bound water. Ann. N.Y. Acad. Sci. 125: 344-354, 1965.

(20) Kell, D.B. and Harris, C.M.: On the dielectrically observable conseuqences of the diffusional motions of lipids and proteins in membranes. Eur. Biophys. J. 12: 181-197, 1985.

(21) Arnold, W.M., Wendt, B., Zimmermann, U. and Korenstein, R.: Rotation of a single swollen thylakoid vesicle in a rotating field. Electrical properties of the photosynthetic membrane and their modification by ionophores, lipophilic ions and pH. Biochim. Biophys. Acta 813: 117-131, 1985.

(22) Bone, S. and Pethig, R.: Cyclodextrins as model systems for the study of proton transport. Int. J. Quantum Chem. Quantum Biol. Symp. 10: 133-141, 1983.

(23) Careri, G., Garaci, M., Giansanti, A. and Rupley, J.A.: Protonic conductivity of hydrated lysozyme powders at megahertz frequencies. Proc. Natl. Acad. Sci. USA 82: 5342-5346, 1985.

(24) Morgan, H. and Pethig, R.: Protonic and ionic conduction in lysozyme. J. Chem. Soc. Faraday I 82: 143-156, 1986.

(25) Gould, J.L.: Magnetic field sensitivity in animals. Annu. Rev. Physiol. 46, 1984.

(26) Grant, E.H., Sheppard, R.J. and South, G.P.: Dielectric Behaviour of Biological Molecules in Solution. Clarendon, Oxford, 1978.

(27) Pethig, R.: Dielectric and Electronic Properties of BIological Materials. Wiley, Chichester, 1979.

(28) Schwan, H.P.: Electrical properties of tissue and cell suspensions. Adv. Biol. Med. Phys. 5: 147-209, 1957.

(29) Almers, W.: Gating currents and charge movements in excitable membranes. Rev. Physiol. Biochem. Pharmacol. 82: 96-190, 1978.

(30) Cole, K.S.: Membranes, Ions and Impulses. University of California Press, Berkeley, 1972.

(31) Schanne, O.F. and Baker, L.E.: Impedance Measurements in Biological Cells. Wiley, New York, 1978.

(32) Geddes, L.A. and Baker, L.E.: The specific resistance of biological material: a compendium of data for the biomedical engineer and physiologist. Med. Biol. Eng. 5: 271-293, 1967.

(33) Stuchley, M.A. and Stuchley, S.S.: Dielectric properties of biological substances—tabulated. J. Microwave Power 15: 19-26, 1980.

(34) Kirkwood, J.G.: Theory of solutions of molecules containing widely separated charges with special application to zwitterions. J. Chem. Phys. 2: 351-361, 1932.

(35) Kirkwood, J.G.: The dielectric polarization of polar liquids. J. Chem. Phys. 7: 911-919, 1939.

(36) Wyman, J.: Dielectric constants of polar solutions. J. Am. Chem. Soc. 56: 536-544, 1934.

(37) Dunning, W.J. and Shutt, W.J.: The dielectric constants of zwitterions and polar molecules as related to pH. Trans. Faraday Soc. 34: 479-485, 1938.

(38) Sheridan, R.P., Levy, R.M. and Salemme, F.R.: Alpha-helix dipole model and electrostatic stabilization of 4-alpha-helical proteins. Proc. Natl. Acad. Sci. USA 79: 4545-4549, 1982.

(39) Essex, C.G., Symonds, M.S., Sheppard, R.J., Grant, E.H., Lamote, R., Soetweey, F., Rosseneu, M.Y. and Peeters, H.: Five component dielectric dispersion in bovine serum albumin solution. Phys. Med. Biol. 22: 1160-1167, 1977.

(40) Hanss, M.: Mesure de la dispersion dielectrique en tres basse frequence de solution de

DNA. Biopolymers 4: 1035-1042, 1966.

(41) Takashima, S.: Dielectric dispersion of deoxyribonucleic acid. J. Mol. Biol. 7: 455-458, 1963.

(42) Takashima, S.: Dielectric dispersion of deoxyribonucleic acid II. J. Phys. Chem. 70: 1372-1377, 1966.

(43) Takashima, S.: Mechanism of dielectric relaxation of deoxyribonucleic acid. Adv. Chem. Ser. 63: 232-244, 1967.

(44) Mandel, M.: Dielectric properties of charged linear macromolecules with particular reference to DNA. Ann. N.Y. Acad. Sci. 74: 303-311, 1977.

(45) Takashima, S., Gabriel, C., Sheppard, R.J. and Grant, E.H.: Dielectric behavior of DNA solution at radio and microwave frequencies (at 20°C). Biophys. J. 46: 29-34, 1984.

(46) Swicord, M.L. and Davis, C.C.: Microwave absorption of DNA between 8 and 12 GHz. Biopolymers 21: 2453-2460, 1982.

(47) Swicord, M.L. and Davis, C.C.: An optical method for investigating the microwave absorption characteristics of DNA and other biomolecules. Bioelectromagnetics 4: 21-42, 1983.

(48) Edwards, G.S., Davis, C.C., Saffer, J.D. and Swicord, M.L.: Resonant microwave absorption of selected DNA molecules. Phys. Rev. Lett. 53: 1284-1287, 1984.

(49) Edwards, G.S., Davis, C.C., Saffer, J.D. and Swicord, M.L.: Microwave-field-driven acoustic modes in DNA. Biophys. J. 47: 799-807, 1985.

(50) Lee, B. and Richards, F.M.: The interpretation of protein structures: estimation of static accessibility. J. Mol. Biol. 55: 379-400, 1971.

(51) Lee, C.Y., McCammon, J.A. and Rossky, P.J.: The structure of liquid water at an extended hydrophobic surface. J. Chem. Phys. 80: 4448-4455, 1984.

(52) Hallenga, K., Grigera, J.R. and Berendsen, H.J.C.: Influence of hydrophobic solutes on the dynamic behaviour of water. J. Phys. Chem. 84: 2381-2390, 1980.

(53) Buchanan, T.J., Haggis, G.H., Hasted, J.B. and Robinson, B.G.: The dielectric estimation of protein hydration. Proc. R. Soc. Lond. A213: 379-391, 1952.

(54) Bone, S., Eden, J. and Pethig, R.: Electrical properties of proteins as a function of hydration and NaCl content. Int. J. Quantum Chem. Quantum Biol. Symp. 8: 307-316, 1981.

(55) Bone, S., Gascoyne, P.R.C. and Pethig, R.: Dielectric properties of hydrated proteins at 9.9 GHz. J. Chem. Soc. Faraday Trans. I 73: 1605-1611, 1977.

(56) Bone, S. and Pethig, R.: Dielectric studies of the binding of water to lysozyme. J. Mol. Biol. 157: 571-575, 1982.

(57) Bone, S. and Pethig, R.: Dielectric studies of protein hydration and hydration-induced flexibility. J. Mol. Biol. 181: 323-326, 1985.

(58) Cross, T.E. and Pethig, R.: Microwave studies of the interactin of DNA and water in the temperature range 90–300K. Int. J. Quantum Chem. Quantum Biol. Symp. 10: 143-152, 1983.

(59) Clementi, E. Structure of water and counterions for nucleic acids in solution. In: Clementi, E. and Sarma, R.H. eds., Structure and Dynamics: Nucleic Acids and Proteins. Adenine Press, New York, 1983.

(60) Careri, G., Gratton, E., Yang, P.H. and Rupley, J.A.: Correlation of IR spectroscopic, heat capacity, diamagnetic susceptibility and enzymatic measurements on lysozyme powder. Nature 284: 572-573, 1980.

(61) Gascoyne, P.R.C., Pethig, R. and Szent-Györgyi, A.: Water structure dependent charge transport in proteins. Proc. Natl. Acad. Sci. USA 78: 261-265, 1981.

(62) Behi, J., Bone, S., Morgan, H. and Pethig, R.: Effect of deuterium-hydrogen exchange on teh electrical conduction in lysozyme. Int. J. Quantum Chem. Quantum Biol. Symp. 9: 367-374, 1982.

(63) Tien, H.T. and Diana, A.L.: Biomolecular lipid membranes: a review and a summary of some recent studies. Chem. Phys. Lipids 2: 55-101, 1968.

(64) Klee, M. and Plonsey, R.: Extracellular stimulation of a cell having a non-uniform membrane. IEEE Trans. Biomed. Eng. BME-21: 452-460, 1974.

(65) Zimmermann, U.: Electric field-mediated fusion and related electrical phenomena. Biochim. Biophys. Acta 694: 227-277, 1982.

(66) Harris, C.M. and Kell, D.B.: On the dielectrically observable consequences of the diffusional motions of lipids and proteins in membranes. Eur. Biophys. J. 13: 11-24, 1985.

(67) Poo, M.-m.: *In situ* electrophoresis of membrane components. Ann. Rev. Biophys. Bioeng. 10: 245-276, 1981.

(68) Singh, B., Smith, C.W. and Hughes, R.: *In vivo* dielectric spectrometer. Med. Biol. Eng. Comput. 17: 45-60, 1979.

(69) Kosterich, J.D., Foster, K.R. and Pollack, S.R.: Dielectric permittivity and electrical conductivity of fluid saturated bone. IEEE Trans. Biomed. Eng. BME-30: 81-86, 1983.

(70) Schwan, H.P.: Die elektrischen eigenschaften von muskelgewebe bei niederfrequenz. Z. Naturforsch. 9b: 245-251, 1954.

(71) Pauly, H. and Schwan, H.P.: The dielectric properties of bovine eye lens. IEEE Trans. Biomed. Eng. BME-11: 103-109, 1964.

(72) Schwan, H.P. and Foster, K.R.: Microwave dielectric properties of tissues: some comments on the rotational mobility of tissue water. Biophys. J. 17: 193-197, 1977.

(73) Foster, K.R., Schepps, J.L., Stoy, R.D. and Schwan, H.P.: Dielectric properties of brain tissue between 0.01 and 10 GHz. Phys. Med. Biol. 24: 1177-1187, 1979.

(74) Rosendal, T.: Concluding studies on the conducting properties of human skin to alternating current. Acta Physiol. Scand. 9: 39-46, 1945.

(75) Yamamoto, T. and Yamamoto, Y.: Dielectric constant and resistivity of epidermal stratum corneum. Med. Biol. Eng. 14: 494-499, 1976.

(76) Clar, E.J., Cambrai, M. and Sturelle, C.: Study of skin horny layer hydration and restoration by impecdance measurement. Cosmetics & Toiletries 97: 33-40, 1982.

(77) Lin, J.C.: Microwave properties of fresh mammalian brain tissues at bdy temporature. IEEE Trans. Biomed. Eng. BME-22: 74-76, 1975.

(78) Stoy, R.D., Foster, K.R. and Schwan, H.P.: Dielectric properties of mammalian tissues from 0.1 to 100 MHz: a summary of recent data. Phys. Med. Biol. 27: 501-513, 1982.

(79) Stuchley, M.A., Kraszewski, A., Stuchly, S.S. and Smith, A.M.: Dielectric properties of animal tissues *in vivo* at radio microwave frequencies: comparison between species. Phys. Med. Biol. 7: 927-936, 1982.

(80) Brady, M.M., Symons, S.A. and Stuchly, S.S.: Dielectric behavior of selected animal tissues *in vitro* at frequencies from 2 to 4 GHz. IEEE Trans. Biomed. Eng. BME-28: 305-307, 1981.

(81) Schwan, H.P. Biophysics of diathermy. In: Licht, S. ed., Therapeutic Heat and Cold. Waverley Press, Baltimore, 63-125, 1965.

(82) Hahn, G.M., Kernahan, A., Martinez, A., Pounds, D. and Prionas, S.: Some heat transfer problems associated with heating by ultrasound, microwaves or radio frequency. Ann. N.Y. Acad. Sci. 335: 327-346, 1980.

(83) Schepps, J.L. and Foster, K.R.: The UHF and microwave dielectric properties of normal and tumour tissues. Variation in dielectric properties with tissue water content. Phys. Med. Biol. 25: 1149-1159, 1980.

(84) Gabriel, C., Sheppard, R.J. and Grant, E.H.: Dielectric properties of ocular tissues at 37°C. Phys. Med. Biol. 28: 43-49, 1983.

(85) Fricke, H. and Morse, S.: The electric capacity of tumors of the breast. J. Cancer Res. 10: 340-346, 1926.

(86) Bottomley, P.A. and Andrew, E.R.: RF magnetic field penetration, phase shift and power dissipation in biological tissue: implications for NMR imaging. Phys. Med. Biol. 23: 630-643, 1978.

(87) Rogers, J.A., Sjeppard, R.J., Grant, E.H., Bleehen, N.M. and Honess, D.J.: The dielectric properties of normal and tumour mouse tissue between 50 MHz and 10 GHz. Br. J. Radio 56: 335-338, 1983.

(88) Foster, K.R. and Schepps, J.L.: Dielectric properties of tumor and normal tissues at radio through microwave frequencies. J. Microwave Power 16: 107-119, 1981.

(89) Hazlewood, C.K., Chang, D.C., Nichold, B.L. and Woesner, D.E.: Nuclear magnetic resonance transverse relaxation times of water protons in skeletal muscle. Biophys. J. 14: 583-606, 1974.

(90) Damadian, R. and Cope, F.W.: NMR in cancer. V. Electronic diagnosis of cancer

potassium nuclear magnetic resonance: spin signatures and T1 beat patterns. Physiol. Chem. Phys. 6: 309-322, 1974.

(91) Pool, T.B., Cameron, I.L., Smith, N.K.R. and Sparks, R.L. Intracellular sodium and growth control: a comparison of normal and transformd cells. In: Cameron, I.L. and Pool, T.B. eds., The Transformed Cell. Academic, New York, 1981.

(92) Cone, C.D.: Electroosmotic interactions accompanying mitosis initiation in sarcoma cells *in vitro*. Trans. N.Y. Acad. Sci. 31: 404-427, 1969.

(93) Cone, C.D.: Variation of the transmembrane potential level as a basic mechanism of mitosis control. Oncology 24: 438-470, 1970.

(94) Cone, C.D. and Tongier, M.: Control of somatic cell mitosis by simulated changes in the transmembrane potential level. Oncology 25: 168-182, 1971.

(95) Purdom, L., Ambrose, E.J. and Klein, G.: A correlation between electrical surface charge and some biological characteristics during the stepwise progression of a mouse sarcoma. Nature 181: 1586-1587, 1958.

(96) Ambrose, E.J., James, A.M. and Lowick, J.H.B.: Differences between the electrical charge carried by normal and homologous tumor cells. Nature 177: 576-577, 1969.

(97) Grant, J.P. and Spyrou, N.M.: Complex permittivity differences between normal and pathological tissues: mechanisms and medical significance. J. Bioelectricity 4: 419-458, 1985.

(98) Schaubel, M.K. and Habal, M.B.: Electropotentials of normal tissue. J. Surg. Res. 9: 513-515, 1969.

(99) Schaubel, M.K. and Habal, M.B.: Electropotentials of surgical specimens. Arch. Pathol. 90: 411-415, 1970.

(100) Becker, R.O.: The bioelectric factors in amphibian limb regeneration. J. Bone Joint Surg. 43A: 643-656, 1961.

(101) Burdette, E.C., Cain, F.L. and Seals, J.: *In vivo* probe measurement technique for determining dielectric properties of VHF through microwave frequencies. IEEE Trans. Microwave Theory Tech. MTT-28: 414-427, 1980.